Suppression of Expression of Heat Shock Protein 70 by Gefitinib and Its Contribution to Pulmonary Fibrosis

Takushi Namba[1], Ken-Ichiro Tanaka[1], Tatsuya Hoshino[1], Arata Azuma[2], Tohru Mizushima[1,3]*

1 Graduate School of Medical and Pharmaceutical Sciences, Kumamoto University, Kumamoto, Japan, **2** Division of Respiratory, Infection and Oncology, Department of Internal Medicine, Nippon Medical School, Tokyo, Japan, **3** Department of Analytical Chemistry, Faculty of Pharmacy, Keio University, Tokyo, Japan

Abstract

Drug-induced interstitial lung disease (ILD), particularly pulmonary fibrosis, is of serious clinical concern. Gefitinib, a tyrosine kinase inhibitor of the epidermal growth factor receptor (EGFR), is beneficial as a drug for treating non-small cell lung cancer; however, this drug induces ILD and the molecular mechanisms underpinning this condition remain unclear. We recently reported that expression of heat shock protein 70 (HSP70) protects against bleomycin-induced pulmonary fibrosis, an animal model of pulmonary fibrosis. In this study, we have examined the effects of drugs known to induce ILD clinically on the expression of HSP70 in cultured lung epithelial cells and have found that gefitinib has a suppressive effect. Results of a luciferase reporter assay, pulse-labelling analysis of protein and experiments using an inhibitor of translation or transcription suggest that gefitinib suppresses the expression of HSP70 at the level of translation. Furthermore, the results of experiments with siRNA for Dicer1, an enzyme responsible for synthesis of microRNA, and real-time RT-PCR analysis suggest that some microRNAs are involved in the gefitinib-induced translational inhibition of HSP70. Mutations in the EGFR affect the concentration of gefitinib required for suppressing the expression of HSP70. These results suggest that gefitinib suppresses the translation of HSP70 through an EGFR- and microRNA-mediated mechanism. *In vivo*, while oral administration of gefitinib suppressed the pulmonary expression of HSP70 and exacerbated bleomycin-induced pulmonary fibrosis in wild-type mice, these effects were not as distinct in transgenic mice expressing HSP70. Furthermore, oral co-administration of geranylgeranylacetone (GGA), an inducer of HSP70, suppressed gefitinib-induced exacerbation of bleomycin-induced pulmonary fibrosis. Taken together, these findings suggest that gefitinib-induced exacerbation of bleomycin-induced pulmonary fibrosis is mediated by suppression of pulmonary expression of HSP70 and that an inducer of HSP70 expression, such as GGA, may be therapeutically beneficial for the treatment of gefitinib-induced pulmonary fibrosis.

Citation: Namba T, Tanaka K-I, Hoshino T, Azuma A, Mizushima T (2011) Suppression of Expression of Heat Shock Protein 70 by Gefitinib and Its Contribution to Pulmonary Fibrosis. PLoS ONE 6(11): e27296. doi:10.1371/journal.pone.0027296

Editor: Kaustubh Datta, University of Nebraska Medical Center, United States of America

Received August 10, 2011; **Accepted** October 13, 2011; **Published** November 9, 2011

Funding: This work was supported by Grants-in-Aid of Scientific Research from the Ministry of Health, Labour, and Welfare of Japan (http://www.mhlw.go.jp/english/index.html), Grants-in-Aid for Scientific Research from the Ministry of Education, Culture, Sports, Science and Technology of Japan (http://www.mext.go.jp/), and Grants-in-Aid of the Japan Science and Technology Agency (http://www.jst.go.jp/). The funders had no role in study design, data collection and analysis, decision to publish, or preparation of the manuscript.

Competing Interests: The authors have declared that no competing interests exist.

* E-mail: mizu@gpo.kumamoto-u.ac.jp

Introduction

Interstitial lung disease (ILD), in particular interstitial pneumonia associated with pulmonary fibrosis, is a devastating chronic lung condition with poor prognosis. Pulmonary fibrosis progresses insidiously, with acute exacerbation of interstitial pneumonia being a highly lethal clinical event [1], [2]. Although most cases of pulmonary fibrosis are idiopathic, some are due to drug side effects (drug-induced pulmonary fibrosis). For example, the anti-tumour drugs gefitinib and imatinib, as well as anti-rheumatoid arthritis drugs such as leflunomide, are known to induce ILD (pulmonary fibrosis). This is cause for serious clinical concern, as it restricts the therapeutic use of these drugs [3], [4], [5]. Unfortunately, the etiology of drug-induced ILD (pulmonary fibrosis) is not yet understood and, as a result, an appropriate animal model has not yet been established. Understanding the mechanism governing drug-induced ILD (pulmonary fibrosis) and developing a viable animal model are therefore important to establish not only a clinical protocol for its treatment but also an assay system that will facilitate screening in order to eliminate candidate drugs with the potential to produce this type of side effect. Bleomycin-induced pulmonary fibrosis in animals mimics some characteristics of human pulmonary fibrosis [6]. We recently reported that leflunomide exacerbates bleomycin-induced pulmonary fibrosis, proposed that this model is a suitable animal model for drug-induced ILD, and suggested that this exacerbation is mediated by epithelial-mesenchymal transition (EMT) of lung epithelial cells [7]. However, the molecular mechanisms underpinning ILD (pulmonary fibrosis) induced by drugs other than leflunomide remain unclear.

Pulmonary fibrosis is induced by repeated epithelial cell damage by reactive oxygen species (ROS) and other stressors and abnormal wound repair and remodelling, resulting in abnormal deposition of extracellular matrix (ECM) proteins, such as collagen. In addition to the increase in transforming growth factor (TGF)-β1 [8], an increase in the level of lung myofibroblasts has been suggested to play an important role in pulmonary fibrosis [9]. It was previously believed that the sole origin of myofibroblasts is

peribronchiolar and perivascular fibroblasts that transdifferentiate into myofibroblasts [10]. However, recently, it was revealed that some of the lung myofibroblasts in pulmonary fibrosis patients originate from lung epithelial cells via EMT [11], [12], [13], [14].

Gefitinib, a tyrosine kinase inhibitor of the epidermal growth factor receptor (EGFR), is a new molecular target agent for the treatment of patients with advanced non-small cell lung cancer who fail to respond to chemotherapy [15]. Furthermore, recent clinical studies have shown that this drug is particularly effective for patients with EGFR mutations, which causes constitutive activation of EGFR-dependent intracellular signal transduction [16], [17]. Although gefitinib has been recognised as relatively safe based on data from clinical trials, post-marketing surveillance of patients prescribed with gefitinib in Japan has revealed that 6.8% of patients developed interstitial pneumonia and that, of these, 40% of the patients died [4], [18], [19]. The incidence of gefitinib-induced ILD and its mortality rate are higher in Japan than in Western countries [20], [21]. However, the mechanism governing gefitinib-induced ILD (pulmonary fibrosis) and the reason for this ethnic difference is unknown. Furthermore, contradictory results have been reported regarding the effect of gefitinib on bleomycin-induced pulmonary fibrosis in animals (prevention and exacerbation) [22], [23] and the mechanisms governing these phenomena are unknown.

Different stressors induce cells to express heat shock proteins (HSPs) through transcriptional regulation mediated by a transcription factor, heat shock factor 1 (HSF1), and a *cis*-element located in the *hsp* gene promoter, heat shock element (HSE) [24]. HSPs, especially HSP70, expressed in cultured cells protect these cells against a range of stressors, including ROS, by refolding or degrading denatured proteins produced by the stressors (HSPs function as molecular chaperones) [24], [25]. Interestingly, geranylgeranylacetone (GGA), a leading anti-ulcer drug on the Japanese market, has been reported to be a non-toxic HSP-inducer [26], [27]. In addition to the cytoprotective effects of HSP70, its anti-inflammatory effects have been identified recently [28]. We have shown that through the cytoprotective, anti-inflammatory and molecular chaperone activities, both genetic and pharmacologic (by GGA) induction of expression of HSP70 is protective in animal models of various diseases, such as gastric and small intestinal lesions, inflammatory bowel diseases, ultraviolet light-induced skin damage and Alzheimer's disease [29], [30], [31], [32], [33], [34]. Furthermore, we recently reported that bleomycin-induced lung injury, inflammation, fibrosis and dysfunction are suppressed in transgenic mice expressing HSP70 or in GGA-administered wild-type mice. We also suggested that HSP70 plays this protective role through cytoprotective and inflammatory effects and by inhibiting the production of TGF-β1 and TGF-β1-dependent EMT of lung epithelial cells [35].

As a mechanism for the regulation of gene expression, microRNAs (miRNAs) have been paid much attention recently. miRNAs are short non-coding single-stranded RNA species which bind to complementary regions of the 3' untranslated regions (UTRs) of mRNA resulting in repression of translation and/or stimulation of degradation of mRNA. Primary miRNA transcripts are first processed in the nucleus to produce hairpin RNAs (pre-miRNAs), which are then exported into the cytoplasm, where Dicer1 cuts the hairpin to produce miRNAs [36]. Aberrant expression of miRNAs is associated with pathologic conditions, such as cancer, diabetes and fibrosis [36,37].

In this study, we examined the effect on the expression of HSP70 of drugs known to induce ILD clinically in cultured lung epithelial cells, and found that gefitinib suppresses the expression of HSP70. The results suggest that gefitinib regulates expression of HSP70 at the level of translation through an EGFR- and miRNA-mediated mechanism. We also found that oral administration of gefitinib suppresses pulmonary expression of HSP70 and suggested that this suppression is involved in gefitinib-induced exacerbation of bleomycin-induced pulmonary fibrosis. These results suggest that HSP70 plays an important role in gefitinib-induced ILD (pulmonary fibrosis) and that examination of the effect of drugs on HSP70-expression *in vitro* is useful as a screening system in order to eliminate candidate drugs with the potential to induce ILD.

Materials and Methods

Ethics Statement

The experiments and procedures described here were carried out in accordance with the Guide for the Care and Use of Laboratory Animals as adopted and promulgated by the National Institutes of Health, and were approved by the Animal Care Committee of Kumamoto University. Permit numbers or approval ID for this study is C-20–166-R1.

Chemicals and animals

Paraformaldehyde, fetal bovine serum (FBS), 4-(dimethylamino)-benzaldehyde (DMBA), chloramine T, cycloheximide, SP600125, Orange G, RPMI1640 and DMEM were obtained from Sigma (St. Louis, MO). Bleomycin was purchased from Nippon Kayaku (Tokyo, Japan). An RNeasy kit, miScript miRNA Mimic and HiPerFect were obtained from Qiagen (Valencia, CA), the PrimeScript® 1st strand cDNA synthesis kit was from TAKARA Bio (Ohtsu, Japan), and the iQ SYBR Green Supermix was from Bio-Rad (Hercules, CA). The mirVana miRNA isolation kit and pMIR-REPORT System were purchased from Applied Biosystems (Carlsbad, CA). Antibodies against actin and HSP70 were purchased from Santa Cruz Biotechnology, Inc. (Santa Cruz, CA) and BD Bioscience (San Francisco, CA), respectively. Antibodies against HSP27, HSP47, HSP60 and HSP90 were from Stressgene (San Francisco, CA). The NCode VILO miRNA cDNA synthesis kit and Lipofectamine (TM2000) were obtained from Invitrogen (Carlsbad, CA). A771726, gefitinib, imatinib, amiodarone, L-hydroxyproline, azophloxin and aniline blue were from WAKO Pure Chemicals (Tokyo, Japan). Xylidine ponceau was from WALDECK GmbH & Co. (Muenster, Germany), and Mayer's hematoxylin, 1% eosin alcohol solution, mounting medium for histological examination (malinol) and Weigert's iron hematoxylin were from MUTO Pure Chemicals (Tokyo, Japan). Transgenic mice expressing HSP70 were gifts from Drs. CE Angelidis and GN Pagoulatos (University of Ioannina, Ioannina, Greece) and were crossed with C57BL/6J wild-type mice 10 times to generate the mice used in this study [32].

Cell culture

A549 and H1975 cells, and PC9 cells were cultured in DMEM and RPMI1640 medium, respectively, supplemented with 10% FBS, 100 U/ml penicillin and 100 μg/ml streptomycin in a humidified atmosphere of 95% air with 5% CO_2 at 37°C.

Real-time RT-PCR analysis

Real-time RT-PCR was performed as previously described [38] with some modifications. Total RNA was extracted from cells using an RNeasy kit or mirVana miRNA isolation kit according to the manufacturer's protocol. Samples were reverse-transcribed using a first-strand cDNA synthesis kit or NCode VILO miRNA cDNA synthesis kit. Synthesized cDNA was used in real-time RT-PCR experiments (Chromo 4 instrument; Bio-Rad Laboratories) using iQ SYBR GREEN Supermix, and analyzed with Opticon

Monitor Software. Specificity was confirmed by electrophoretic analysis of the reaction products and by the inclusion of template- or reverse transcriptase-free controls. To normalize the amount of total RNA present in each reaction, *actin* or RUN44 cDNA was used as an internal standard. Primers were designed using the Primer3 website or NCode™ miRNA database website.

The primers used were (name: forward primer, reverse primer): *hsp27*: 5'-ccacccaagtttcctcctc-3', 5'-gactgggatggtgatctcgt-3'; *hsp47*: 5'-ccatgttcttcaagccacact-3', 5'-cgtagtagttgtagaggcctgt-3'; *hsp60*: 5'-tttcagatggagtggctgtg-3', 5'-caatgccttcttcaacagca-3'; *hsp70*: 5'-aggccaacaagatcaccatc-3', 5'-tcgtcctccgctttgtactt-3'; *hsp90*: 5'-ggcagaggctgataagaacg-3', 5'-ctggggatcttccagactga-3'; *actin*: 5'-ggacttcgagcaagagatgg-3', 5'- agcactgtgttggcgtacag-3'; miR-146a: 5'-tgagaactgaattccatgggtt-3'; miR-146b-5p: 5'-gtgagaactgaattccataggct-3'; miR-223*: 5'-gcgtgtatttgacaagctgagtt-3'; miR-561: 5'-cgcaaagtttaagatccttgaagt-3'; miR-449a: 5'-tggcagtgtattgttagctggt-3'; miR-449b: 5'-aggcagtgtattgttagctggc-3'; RUN44: 5'-gagctaattaagaccttcatgttca-3', 5'-cctggatgatgataagcaaatg-3'. For miRNAs, the universal primer in the NCode VILO miRNA cDNA synthesis kit was used as the reverse primer.

We searched for miRNAs that potentially bind to the 3' UTR of *hsp70*, using the TargetScan and Segal Lab websites.

Luciferase assay

DNA fragments of the *hsp70* 3' UTR (from 2169 to 2427) were amplified by PCR and ligated into the Spe*I*-Hin*dIII* site of the *Photinus pyralis* luciferase reporter plasmid (pMIR-REPORT) to generate pMIR/luc/*hsp70* 3' UTR. The pGL-3/HSE plasmid was constructed by inserting HSE just upstream of the *luciferase* gene. The pGL-3/*hsp70*pro plasmid, which was constructed by inserting the *hsp70* promoter into the same region, was generously provided by Dr. Chang EB (University of Chicago). The luciferase assay was performed as described previously [38]. Transfections were carried out using Lipofectamine (TM2000) according to the manufacturer's instructions. Cells were used for experiments after a 24 h recovery period. Transfection efficiency was determined in parallel plates by transfection of cells with a pEGFP-N1 control vector. Cells were transfected with 0.5 μg of one of the *Photinus pyralis* luciferase reporter plasmids (pMIR/luc/*hsp70* 3' UTR, pGL-3/*hsp70*pro or pGL-3/HSE) and 0.125 μg of the internal standard plasmid bearing the *Renilla reniformis* luciferase reporter (pRL-SV40). *Photinus pyralis* luciferase activity in the cell extracts was measured using the Dual Luciferase Assay System and then normalized for *Renilla reniformis* luciferase activity.

Immunoblotting analysis

Whole cell extracts were prepared as described previously [38]. The protein concentration of the samples was determined by the Bradford method [39]. Samples were applied to polyacrylamide SDS gels, subjected to electrophoresis, and the resultant proteins immunoblotted with their respective antibodies.

Pulse-chase and pulse-labelling analyses

Pulse-chase and pulse-labelling analyses were carried out as described previously [40], with some modifications. Cells were labelled with [^{35}S]methionine and [^{35}S]cysteine in methionine- and cysteine-free RPMI1640 medium for 15 min. To chase labelled proteins, cells were washed with fresh complete (with methionine and cysteine) medium three times and incubated in complete medium for 4 or 8 h. HSP70 was immunoprecipitated with its antibody and separated by SDS-polyacrylamide gel electrophoresis, and visualised by autoradiography (Fuji BAS 2500 imaging analyzer).

Transfection of cells with siRNA or miRNA mimic RNA fragments

The siRNA for Dicer1 and the miRNA mimic RNA fragments for miR-146a and miR-146b-5p were purchased from Qiagen. A549 cells were transfected with these RNAs using HiPerFect transfection reagents according to the manufacturer's instructions. The siRNA (5'-uucuccgaacgugucacgudTdT-3' and 5'-acgugacacguucggagaadTdT-3') was used as a non-specific siRNA.

Administration of bleomycin, gefitinib and GGA

C57BL/6 mice were maintained under chloral hydrate anesthesia (500 mg/kg) and given one intratracheal injection of bleomycin (1 or 2 mg/kg) to induce fibrosis. Gefitinib (200 mg/kg) was dissolved in 1% methylcellulose and administered orally. GGA (200 mg/kg) was dissolved in 5% arabic gum and 0.06% Tween and administered orally.

Histological analysis

Lung tissue samples were fixed in 4% buffered paraformaldehyde and embedded in paraffin before being cut into 4 μm-thick sections.

For histological examination, sections were stained first with Mayer's haematoxylin and then with 1% eosin alcohol solution. Samples were mounted with malinol and inspected with the aid of an Olympus BX51 microscope.

For Masson's trichrome staining of collagen, sections were sequentially treated with solution A (5% (w/v) potassium dichromate and 5% (w/v) trichloroacetic acid), Weigert's iron hematoxylin, solution B (1.25% (w/v) phosphotungstic acid and 1.25% (w/v) phosphomolybdic acid), 0.75% (w/v) Orange G solution, solution C (0.12% (w/v) xylidine ponceau, 0.04% (w/v) acid fuchsin and 0.02% (w/v) azophloxin), 2.5% (w/v) phosphotungstic acid, and finally aniline blue solution. Samples were mounted with malinol and inspected with the aid of an Olympus BX51 microscope.

Hydroxyproline determination

Hydroxyproline content was determined as previously described [41]. Briefly, the right lung was removed and homogenized in 0.5 ml of 5% TCA. After centrifugation, pellets were hydrolyzed in 0.5 ml of 10 N HCl for 16 h at 110°C. Each sample was incubated for 20 min at room temperature after the addition of 0.5 ml of 1.4% (w/v) chloramine T solution and then incubated at 65°C for 10 min after the addition of 0.5 ml of Ehrlich's reagent (1M DMBA, 70% (v/v) isopropanol and 30% (v/v) perchloric acid). Absorbance was measured at 550 nm and the amount of hydroxyproline was determined.

Statistical analysis

Two-way analysis of variance (ANOVA), followed by the Tukey test or the Student's *t*-test for unpaired results, was used to evaluate differences between more than three groups or between two groups, respectively. Differences were considered to be significant for values of $P<0.05$.

Results

Suppression of expression of HSP70 by gefitinib

We first examined the effects of drugs known to induce ILD clinically (A771726 (an active metabolite of leflunomide), amiodarone, gefitinib and imatinib) on the expression of HSP70 in cultured human type II alveolar (A549) cells. As shown in Fig. S1, a decrease in the level of HSP70 was observed in cells treated with gefitinib but not in cells treated with other drugs.

As shown in Fig. 1A, treatment of cells with gefitinib decreased the level of not only HSP70 but also HSP90 in a dose-dependent manner; however, the decrease was only clearly observed for HSP70 and not for HSP90, at the concentration of 1 μM. In contrast, levels of other HSPs (HSP27, HSP47 and HSP60) were not affected by treatment with gefitinib (Fig. 1A). Erlotinib is another inhibitor of EGFR used clinically [42] and here we found that this drug also decreases the levels of HSP70 and HSP90 (Fig. 1B), suggesting that the inhibitory effect of gefitinib on EGFR is involved in the decrease in the level of HSP.

Real-time RT-PCR analysis revealed that treatment of cells with gefitinib at 1 μM, a concentration determined to be sufficient to decrease the level of HSP70 (Fig. 1A), did not affect the *hsp70* mRNA level; however, this drug decreased the level at concentrations higher than 10 μM (Fig. 1C).

Suppression of translation of HSP70 by gefitinib

The cellular level of protein is regulated by various factors, such as transcription, mRNA stability, translation and protein stability. With these possibilities in mind, we then examined which of these factors is affected by gefitinib in relation to HSP70. The results in Fig. 1C suggest that 1 μM gefitinib does not affect the transcription and mRNA stability of *hsp70*.

To confirm this, a luciferase reporter assay was used to examine the effect of gefitinib on the promoter activity of *hsp70*. Treatment of cells with gefitinib did not affect the luciferase activity in cells carrying a reporter plasmid with an *hsp70* promoter or an HSE inserted upstream of the *luciferase* gene (Fig. 2A), suggesting that gefitinib does not affect the promoter activity of *hsp70*. Further to this, 1 μM gefitinib did not affect the *hsp70* mRNA level in cells pre-treated with actinomycin D, an inhibitor of transcription (Fig. 2B), suggesting that treatment of cells with 1 μM gefitinib does not affect *hsp70* mRNA stability. The results in Fig. 1A and B also suggest that treatment of cells with 10 μM gefitinib affects *hsp70* mRNA stability but not promoter activity.

We then tested whether gefitinib affects the translation and degradation of HSP70. As shown in Fig. 2C, the decrease in the level of HSP70 with 1 μM gefitinib was not observed in cells pre-

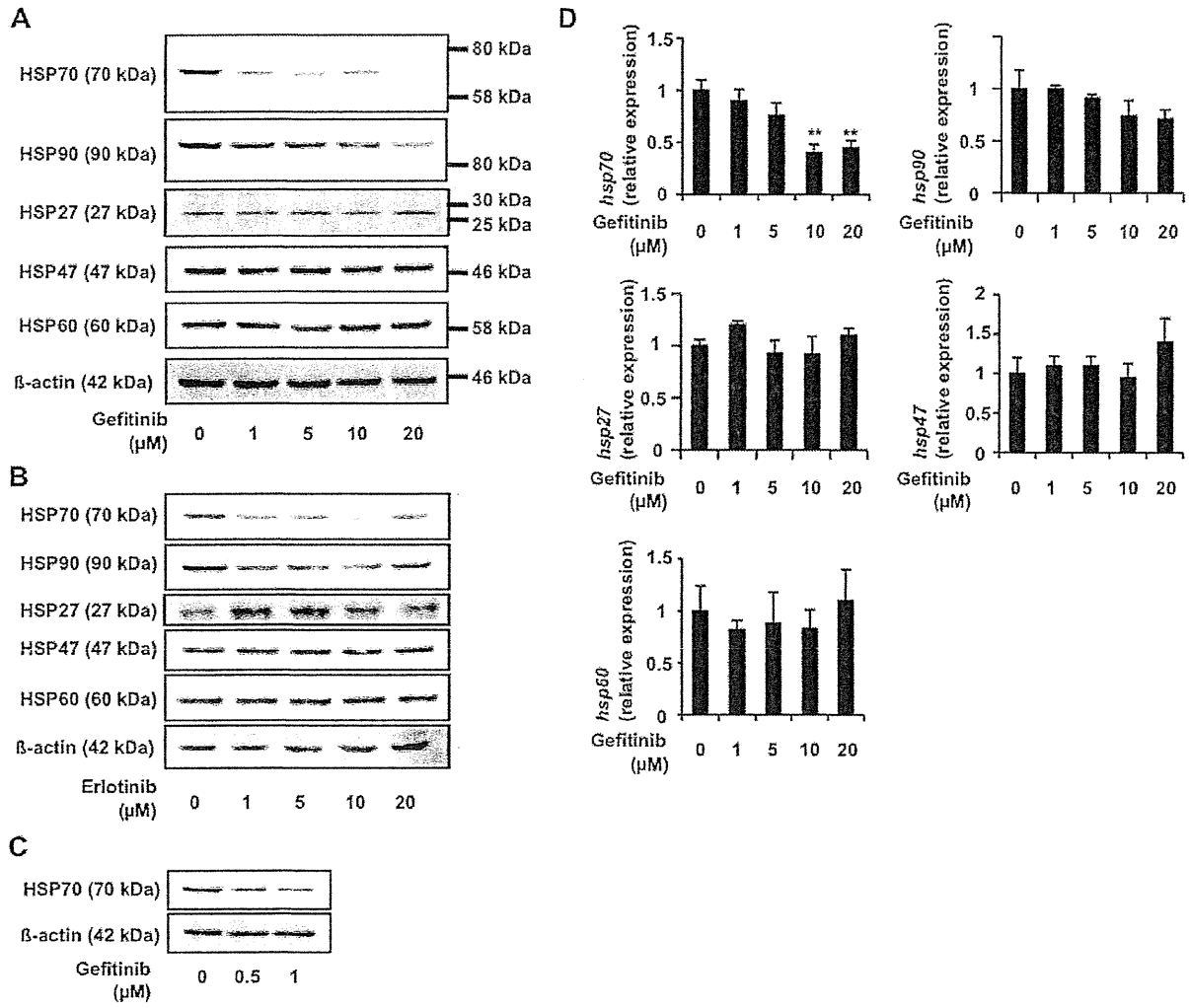

Figure 1. Suppression of expression of HSPs by gefitinib. A549 cells were incubated with the indicated concentration of gefitinib (A, C) or erlotinib (B) for 24 h (A, B) or 12 h (C). Whole-cell extracts were analyzed by immunoblotting with an antibody against HSP70, HSP90, HSP27, HSP47, HSP60 or actin (A, B). Total RNA was extracted and subjected to real-time RT-PCR using a specific primer set for each gene. Values were normalized to the *actin* gene, expressed relative to the control sample (C). Values shown are mean ± S.D. ($n=3$). $^{**}P<0.01$.
doi:10.1371/journal.pone.0027296.g001

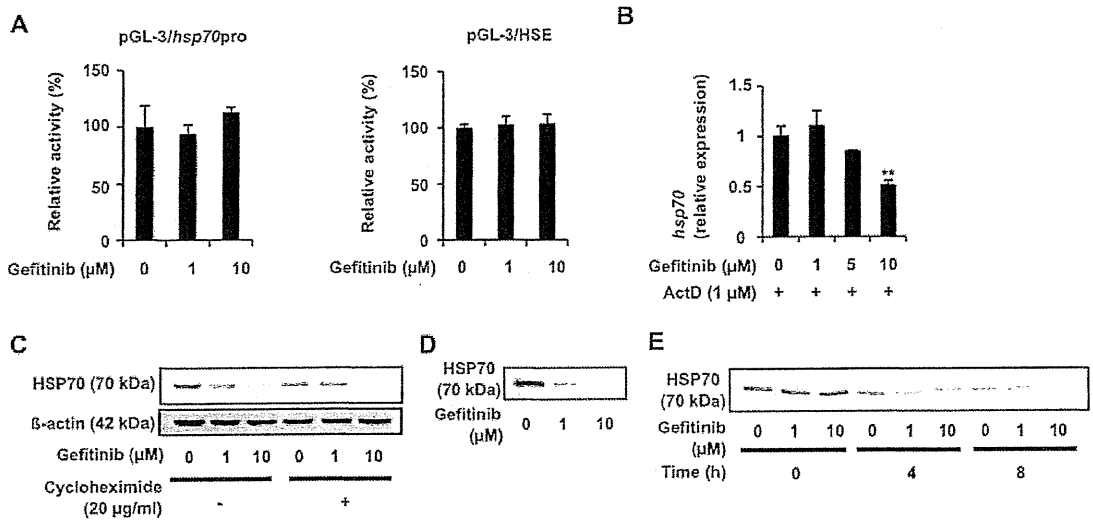

Figure 2. Translational regulation of expression of HSP70 by gefitinib. A549 cells were co-transfected with pRL-SV40 (internal control plasmid carrying the *R. reniformis luciferase* gene) and a pGL-3 derivative (pGL-3/*hsp70*pro or pGL-3/HSE) and cultured for 24 h. Cells were incubated with the indicated concentration of gefitinib for 24 h and *P. pyralis* luciferase activity was measured and normalized for *R. reniformis* luciferase activity. The 100% value of the *P. pyralis* luciferase activity is 6.9×10^4 or 5.8×10^4 units for pGL-3/*hsp70*pro or pGL-3/HSE, respectively (A). A549 cells were pre-incubated with 1 μg/ml actinomycin D (ActD) (B) or 20 μg/ml cycloheximide (C) for 1 h and further incubated for 8 h (B) or 24 h (C) with the indicated concentration of gefitinib (B, C). The mRNA (B) and protein (C) expression was monitored and is expressed as described in the legend of Fig. 1 A549 cells were pulse-labelled for 15 min with [^{35}S]methionine and [^{35}S]cysteine (D, E). Before the pulse-labelling, cells were incubated with the indicated concentration of gefitinib for 8 h (D). Pulse-labelled proteins were chased with excess amounts of Non-radioactively labeled methionine and cysteine for the indicated period in the presence of the indicated concentration of gefitinib (E). Labelled proteins were extracted, immunoprecipitated with antibody against HSP70, subjected to SDS-PAGE and autoradiographed (D, E). Values are mean ± S.D. ($n=3$). **$P<0.01$.
doi:10.1371/journal.pone.0027296.g002

treated with cycloheximide, an inhibitor of protein synthesis. Furthermore, a protein pulse-labelling experiment showed that the synthesis of HSP70 was inhibited in cells pre-treated with gefitinib (Fig. 2D). These results suggest that 1 μM gefitinib inhibits the translation of HSP70. On the other hand, the results of the pulse-chase experiment suggest that treatment of cells with 1 μM gefitinib does not affect the stability of HSP70; 1 μM gefitinib did not affect the level of labelled HSP70 after chase periods of 4 h or 8 h (Fig. 2E). The results in Fig. 2E also suggest that treatment of cells with 10 μM gefitinib stimulates the degradation of HSP70.

3' UTRs of genes play an important role in translational regulation, including that by miRNAs. Thus, we examined the contribution of this region to gefitinib-induced suppression of expression of HSP70 by a luciferase reporter assay. Treatment of cells with gefitinib significantly decreased the luciferase activity in cells carrying the reporter plasmid in which the 3' UTR of *hsp70* was inserted downstream of the *luciferase* gene (Fig. 3A), suggesting that 3' UTR-mediated modulation of HSP70 translation plays an important role in the gefitinib-induced suppression of HSP70 expression.

The contribution of miRNAs to gefitinib-induced suppression of HSP70 expression was then tested by use of siRNA for Dicer1, a protein essential for maturation of miRNAs. As shown in Fig. 3B, transfection of cells with siRNA for Dicer1 decreased the level of *Dicer1* mRNA, but not that of *hsp70*, suggesting that the miRNA system is not involved in the regulation of *hsp70* mRNA stability. The decrease in the level of HSP70 and inhibition of HSP70 protein synthesis in the presence of 1 μM gefitinib were not observed in cells transfected with siRNA for Dicer1 (Fig. 3C and D), suggesting that the 1 μM gefitinib-dependent inhibition of HSP70 translation is mediated by the miRNA system. However, the 10 μM gefitinib-dependent decrease in the level of HSP70 and inhibition of protein synthesis of HSP70 were observed even in cells transfected with siRNA for Dicer1 (Fig. 3C and D).

Next, using a database, we searched for miRNAs with sequences complementary to the 3' UTR of *hsp70*. Six candidate miRNAs were found (miR-146a, miR-146b-5b, miR-223*, miR-561, miR-449a and miR-449b). Real-time RT-PCR analysis revealed that among these miRNAs, the levels of miR-146a and miR-146b-5b clearly increased after treatment of cells with 1 μM gefitinib (we used experimental conditions of real-time RT-PCR under which only fully processed miRNA could be detected) (Fig. 4A). Furthermore, transfection of cells with siRNA for Dicer1 suppressed this gefitinib-dependent increase in the levels of these miRNAs (miR-146a, miR-146b-5b) (Fig. 4B) and transfection of cells with synthesized miR-146a and miR-146b-5b mimic RNA fragments decreased the level of HSP70 (Fig. 4C and D) but not that of *hsp70* mRNA (Fig. 4E). These results suggest that a gefitinib-dependent increase in the levels of miR-146a and miR-146b-5b is involved in gefitinib-dependent inhibition of HSP70 translation.

Involvement of EGFR and JNK inhibition in gefitinib-dependent suppression of expression of HSP70

As described above, gefitinib inhibits self-phosphorylation of tyrosine residues in the cytosolic domains of EGFR. Thus, here we tested whether or not gefitinib suppresses expression of HSP70 through inhibition of the EGFR. To do this we used the cell lines H1975 and PC9 which are resistant or sensitive, respectively, to gefitinib-induced inhibition of the self-phosphorylation of EGFR and the resulting modulation of intracellular signal transduction due to mutations in the EGFR [43], [44]. As shown in Fig. 5A, the concentration of gefitinib required for suppression of HSP70 expression was higher and lower in H1975 cells and PC9 cells,

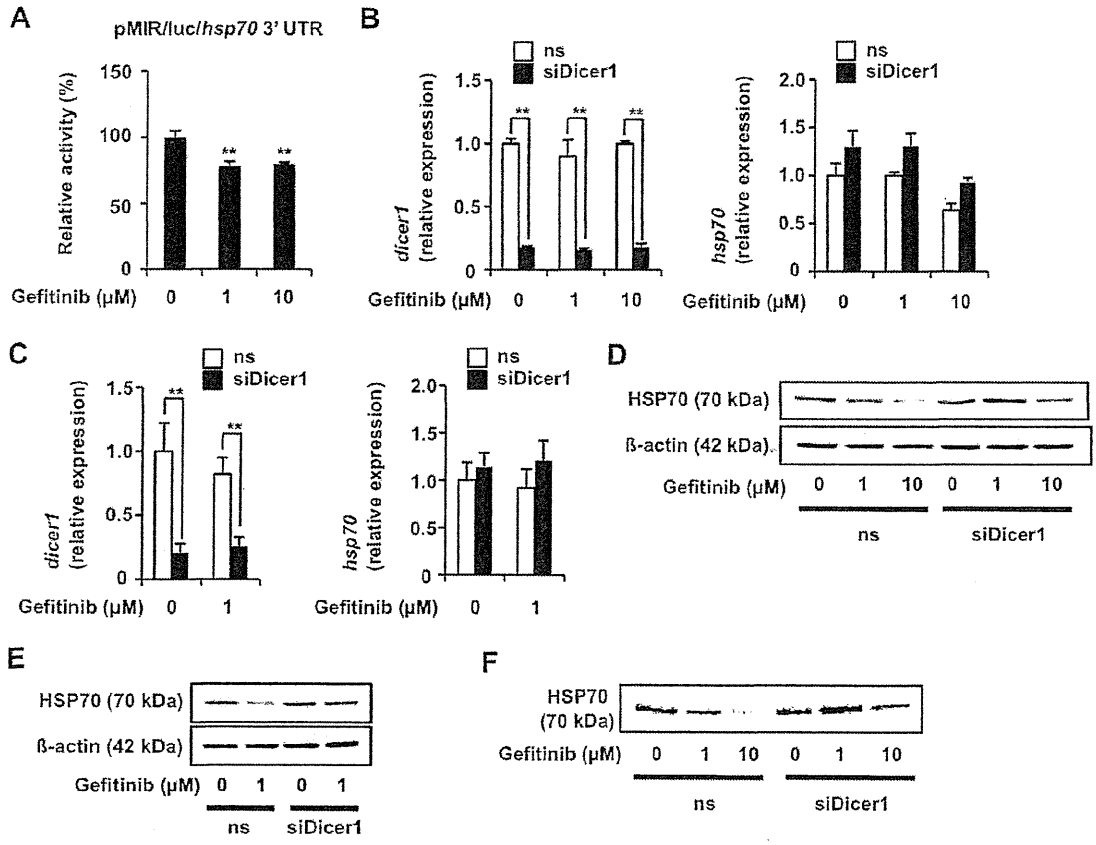

Figure 3. Contribution of miRNA to gefitinib-dependent suppression of expression of HSP70. A549 cells were co-transfected with pRL-SV40 and pMIR/luc/*hsp70* 3' UTR and cultured for 24 h. Cells were incubated with the indicated concentration of gefitinib for 24 h and luciferase reporter assay was done as described in the legend of Fig. 2. The 100% value of the *P. pyralis* luciferase activity is 1.2×10^5 units (A). A549 cells were transfected with siRNA for Dicer1 (siDicer1) or non-specific siRNA (ns) (B-D). After 24 h, cells were incubated with the indicated concentration of gefitinib for 12 h (B), 24 h (C) or 8 h (D). The mRNA (B) and protein (C) expression was monitored and is expressed as described in the legend of Fig. 1. Pulse-labelling experiments were performed as described in the legend of Fig. 2 (D). Values shown are mean ± S.D. ($n=3$). $^{**}P<0.01$; n.s., not significant.

doi:10.1371/journal.pone.0027296.g003

respectively, than for A549 cells, suggesting that gefitinib suppresses expression of HSP70 through an inhibitory effect on the self-phosphorylation of EGFR.

Activation of the EFGR affects various cellular responses through modulation of intracellular signal transduction, such as activation of JNK and ERK [45], [46]. To test whether inhibition of JNK or ERK is involved in gefitinib-dependent suppression of HSP70 expression, we examined the effect of inhibitors of JNK and ERK, SP600125 and U0126, respectively, on the expression of HSP70. Treatment of cells with SP600125 (Fig. 5B) but not U0126 (data not shown) decreased the level of HSP70, suggesting that the inhibition of JNK is involved in the gefitinib-dependent suppression of HSP70 expression.

Effect of gefitinib on bleomycin-induced pulmonary fibrosis

As described in the Introduction, we recently reported that expression of HSP70 protects against bleomycin-induced pulmonary fibrosis [35]. Therefore, the *in vitro* results outlined above imply that gefitinib exacerbates bleomycin-induced pulmonary fibrosis through suppression of HSP70 expression. To test this, we examined the effect of oral daily administration of gefitinib on the expression of HSP70 in the lungs. As shown in Fig. S2, this administration decreases the level of HSP70. The decrease became apparent at day 3 and was also observed at day 6 (Fig. S2). Therefore, to examine the effect of administration of gefitinib on bleomycin-induced pulmonary fibrosis, mice were orally administered gefitinib once per day for three days before receiving a single intratracheal administration of bleomycin; the administration of gefitinib was then continued, once every two days, for the following 14 days.

Histopathological analysis of pulmonary tissue using hematoxylin and eosin (H & E) staining revealed that the simultaneous oral administration of gefitinib (200 mg/kg) and intratracheal administration of bleomycin (1 mg/kg) produced severe pulmonary damage (thickened and edematous alveolar walls and interstitium, and infiltration of leucocytes) (Fig. 6A). Administration of either gefitinib or bleomycin alone did not cause such clear-cut pulmonary damage (Fig. 6A). Masson's trichrome staining of collagen revealed that administration of bleomycin caused slight collagen deposition, an effect that was greatly exacerbated by simultaneous administration of gefitinib (Fig. 6B). The pulmonary hydroxyproline level (an indicator of collagen levels) was increased by administration of bleomycin alone, and this effect was further

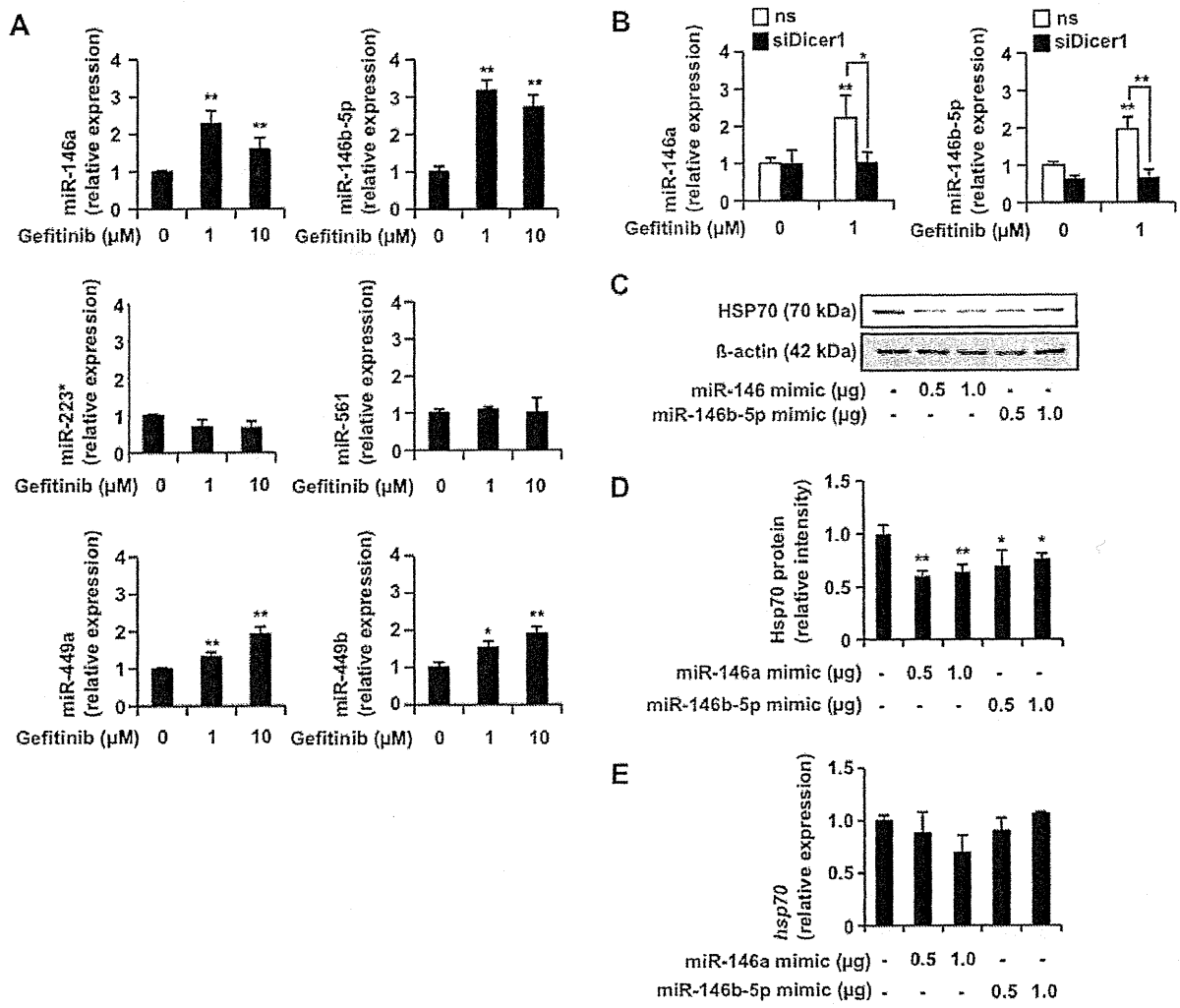

Figure 4. Identification of miRNAs involved in gefitinib-dependent suppression of expression of HSP70. A549 cells were incubated with the indicated concentration of gefitinib for 3 h (A). A549 cells were transfected with siRNA for Dicer1 (siDicer1) or non-specific siRNA (ns) and after 24 h were incubated with the indicated concentration of gefitinib for 3 h (B). A549 cells were transfected with the indicated amount (μg/well) of miRNA mimic RNA fragments for 24 h (C, E). The RNA (A, B, E) and protein (C) expression was monitored and expressed as described in the legend of Fig. 1. The RUN44 non-coding RNA was used for normalization (A, B, E). The intensities of the HSP70 bands were determined and are expressed relative to the control (one of the gels is shown in C) (D). Values shown are mean ± S.D. ($n=3$). $^{**}P<0.01$; $^{*}P<0.05$; n.s., not significant.
doi:10.1371/journal.pone.0027296.g004

enhanced by the simultaneous administration of gefitinib (Fig. 6E). Under our experimental conditions, administration of gefitinib alone did not cause collagen deposition nor increase the level of pulmonary hydroxyproline (Fig. 6B and E).

We also performed similar experiments in transgenic mice expressing HSP70. Since these mice are resistant to bleomycin, we used a higher dose (2 mg/kg) of bleomycin than in the previously described experiments. As shown in Fig. 6C, D and F, the gefitinib-dependent enhancement of bleomycin-induced pulmonary damage, collagen deposition and increase in pulmonary hydroxyproline level were not clearly observed in the transgenic mice, suggesting that gefitinib exacerbates bleomycin-induced pulmonary fibrosis through the suppression of HSP70 expression.

To test this idea, we examined the effect of the administration of gefitinib and/or bleomycin on pulmonary expression of HSP70 in wild-type mice and transgenic mice expressing HSP70. To begin with, we confirmed the overexpression of HSP70 in the lungs of transgenic mice in both the presence and absence of gefitinib administration (Fig. 6G). As shown in Fig. 6H and I, in wild-type mice, administration of gefitinib decreased the pulmonary level of HSP70 in both the presence and absence of simultaneous bleomycin administration. Administration of bleomycin alone also decreased the pulmonary level of HSP70 (Fig. 6H and I). In contrast, such a gefitinib-dependent decrease in the pulmonary level of HSP70 was not observed clearly in transgenic mice expressing HSP70 in both the presence or absence of simultaneous administration of bleomycin (Fig. 6J). We also found that using a lower dose of gefitinib (100 mg/kg) neither exacerbated bleomycin-induced pulmonary fibrosis nor suppressed pulmonary expression of HSP70 (Fig. S3). These results suggest that administration of gefitinib exacerbates bleomycin-induced pulmonary fibrosis through suppression of HSP70 expression.

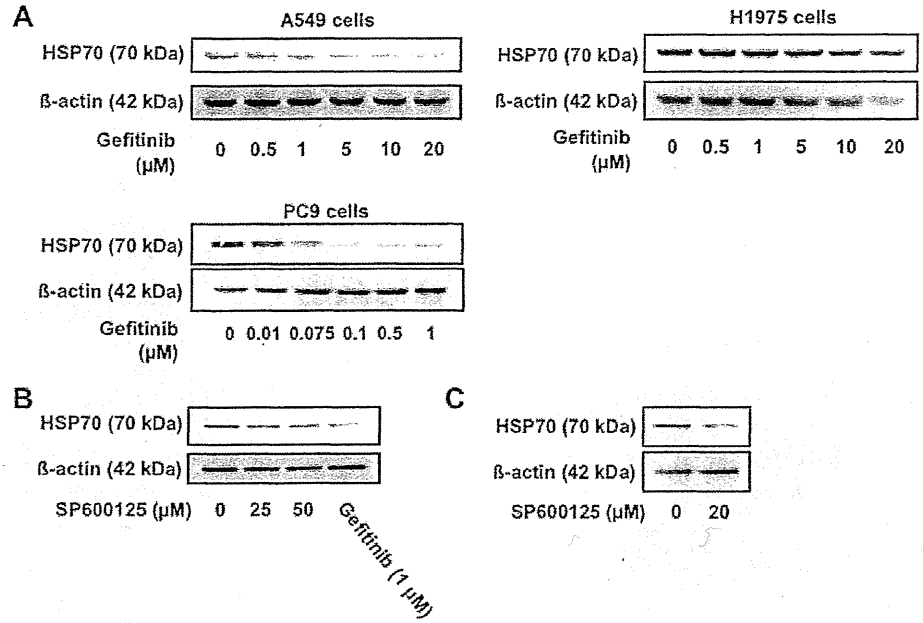

Figure 5. Involvement of inhibition of EGFR and JNK in gefitinib-dependent suppression of expression of HSP70. A549 (A-C) and H1975 and PC9 (A) cells were incubated with the indicated concentration of gefitinib (A, B) or SP600125 (B) for 24 h. Protein expression was monitored and is expressed as described in the legend of Fig. 1.
doi:10.1371/journal.pone.0027296.g005

For further confirmation of this idea, we examined the effect of co-administration of GGA. As shown in Fig. 7A-C, co-administration of GGA clearly suppressed the gefitinib-dependent enhancement of bleomycin-induced pulmonary tissue damage, collagen deposition and increases in the pulmonary hydroxyproline level in wild-type mice. We also examined the effect of GGA on the expression of HSP70 in the lung. As shown in Fig. 7D and E, co-administration of GGA recovered the gefitinib-suppressed expression of HSP70 in the lung, suggesting that GGA suppresses the gefitinib-dependent exacerbation of bleomycin-induced pulmonary fibrosis by inducing the recovery of HSP70 expression.

Discussion

Because the molecular mechanism governing drug-induced ILD (interstitial pneumonia associated with pulmonary fibrosis) is unknown, a suitable animal model is not available at present. Consequently, neither a clinical protocol for the treatment of drug-induced ILD nor an assay system to eliminate candidate drugs with the potential to cause this type of side effect has been established. We recently reported that A771726, an active metabolite of leflunomide, induced EMT of lung epithelial cells both *in vitro* and *in vivo*, and that administration of leflunomide exacerbated bleomycin-induced pulmonary fibrosis, suggesting that the leflunomide-dependent exacerbation of bleomycin-induced pulmonary fibrosis is mediated by the stimulation of EMT of lung epithelial cells. We proposed that examination of the EMT-inducing ability of candidate drugs is useful for screening to eliminate those with the potential side effect of inducing pulmonary fibrosis. We also found that leflunomide-dependent exacerbation of bleomycin-induced pulmonary fibrosis is ameliorated by the simultaneous intratracheal administration of uridine, which suppresses the A771726-dependent induction of EMT *in vitro*, and propose that this administration is beneficial for the treatment of leflunomide-induced pulmonary fibrosis in humans. In the present study, we followed a similar strategy, focusing on the expression of HSP70, because we had recently reported that expression of HSP70 protects against bleomycin-induced pulmonary fibrosis through cytoprotective and anti-inflammatory effects and, by inhibiting the production of TGF-β1 and TGF-β1-dependent EMT of lung epithelial cells [35].

We have found that gefitinib suppresses the expression of HSP70 *in vitro*. The concentration of gefitinib used (1 μM) is similar to that obtained in plasma when administered at therapeutic levels (about 1-2 μM) [47]. Thus, we considered that the suppression of HSP70 expression by gefitinib is clinically relevant and investigated the molecular mechanism underlying this effect. We concluded that treatment of cells with gefitinib (1 μM) decreases the level of HSP70 through inhibition of translation based on observations that (i) the gefitinib-dependent decrease in the level of HSP70 was suppressed by an inhibitor of translation, (ii) the translation of HSP70, measured by pulse-labelling experiments, was inhibited by treatment of cells with gefitinib, and (iii) *hsp70* promoter activity, the level and stability of *hsp70* mRNA and the stability of HSP70 were all unaffected by treatment of cells with gefitinib. Furthermore, we suggested that two miRNAs (miR-146a and miR-146b-5p) are involved in this gefitinib-dependent suppression of HSP70 translation; this was based on our observations that (i) the introduction of the 3' UTR of *hsp70* into a luciferase reporter plasmid caused a gefitinib-dependent decrease in luciferase activity, (ii) the gefitinib-dependent suppression of HSP70 translation was not observed in cells transfected with siRNA for Dicer1, and (iii) gefitinib increased the levels of miR-146a and miR-146b-5p, both of which have the ability to decrease the level of HSP70. Since for various cancer cells and tissues, down-regulation of expression of these miRNAs and up-regulation of HSP70 and the contribution of these to cancer progression have been reported [48], [49], [50], the results

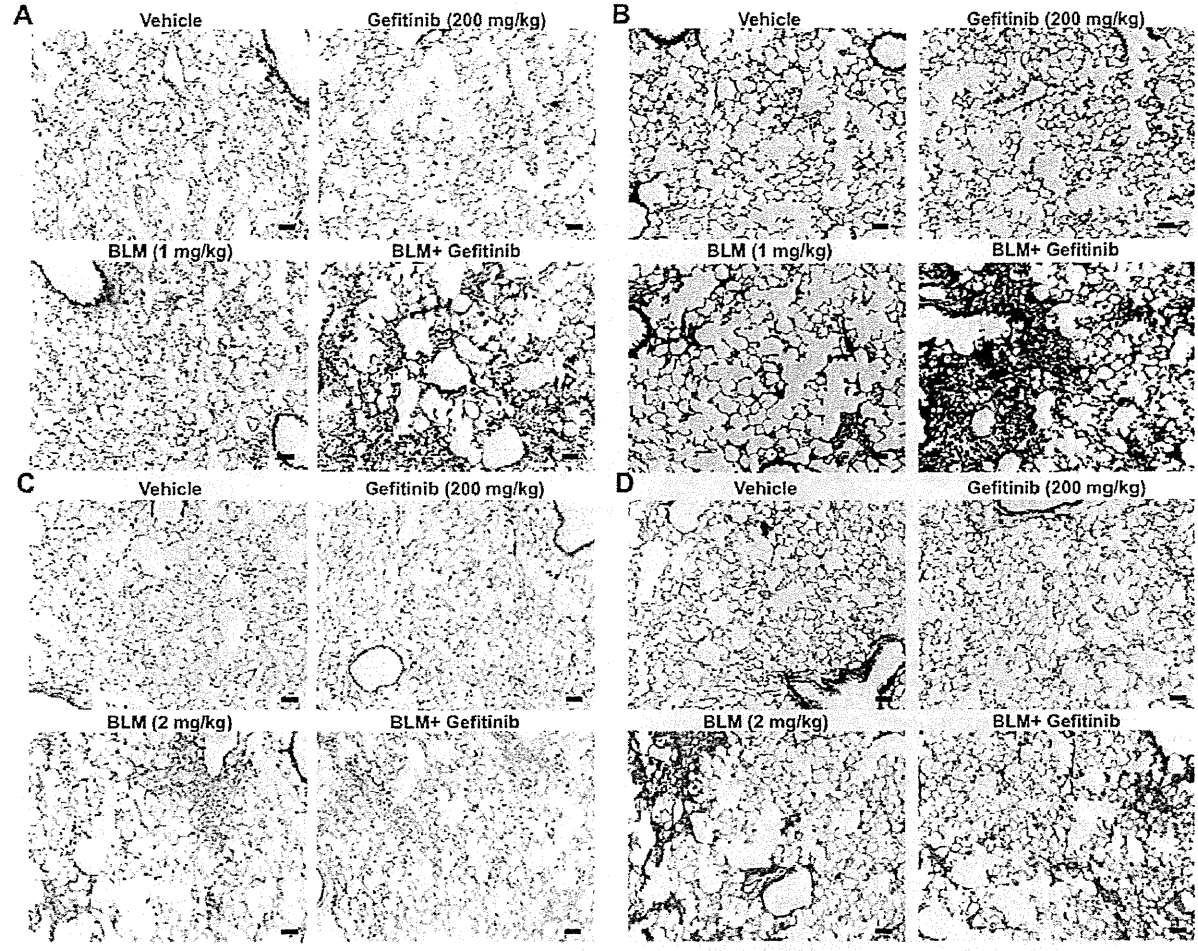
A
Vehicle
Gefitinib (200 mg/kg)
BLM (1 mg/kg)
BLM+ Gefitinib
B
Vehicle
Gefitinib (200 mg/kg)
BLM (1 mg/kg)
BLM+ Gefitinib
C
Vehicle
Gefitinib (200 mg/kg)
BLM (2 mg/kg)
BLM+ Gefitinib
D
Vehicle
Gefitinib (200 mg/kg)
BLM (2 mg/kg)
BLM+ Gefitinib

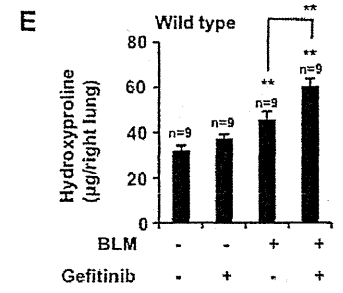
E
Wild type
Hydroxyproline (μg/right lung)
BLM
Gefitinib

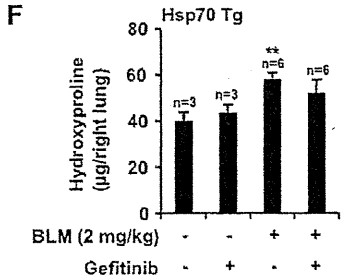
F
Hsp70 Tg
Hydroxyproline (μg/right lung)
BLM (2 mg/kg)
Gefitinib

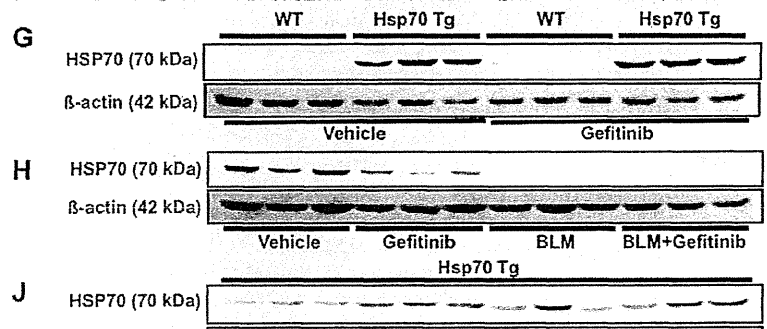
G
WT
Hsp70 Tg
WT
Hsp70 Tg
HSP70 (70 kDa)
ß-actin (42 kDa)
Vehicle
Gefitinib

H
HSP70 (70 kDa)
ß-actin (42 kDa)
Vehicle
Gefitinib
BLM
BLM+Gefitinib

J
Hsp70 Tg
HSP70 (70 kDa)
ß-actin (42 kDa)
Vehicle
Gefitinib
BLM
BLM+Gefitinib

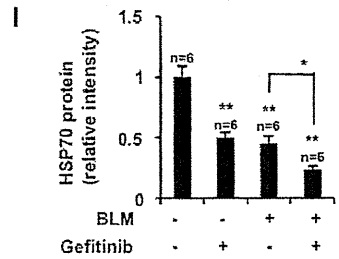
I
HSP70 protein (relative intensity)
BLM
Gefitinib

Figure 6. Effect of gefitinib on bleomycin-induced pulmonary fibrosis and pulmonary expression of HSP70. Wild-type mice (A, B, E, G, H) and transgenic mice expressing HSP70 (C, D, F, G, J) were orally administered gefitinib (200 mg/kg) or vehicle once per day for 3 days (from day 0 to day 2), then treated once only with or without 1 mg/kg (for wild-type mice) or 2 mg/kg (for the transgenic mice) bleomycin (BLM) (day 3). Mice were then orally administered gefitinib (200 mg/kg) or vehicle once per 2 days for 14 days (from day 3 to day 17). Sections of pulmonary tissue were prepared at day 17 and subjected to histological examination (H & E staining (A, C) or Masson's trichrome staining (B, D)) (scale bar, 50 μm) (A-D). Pulmonary hydroxyproline levels at day 17 were determined (E, F). Total protein was extracted from pulmonary tissues at day 17 and analyzed by immunoblotting with an antibody against HSP70 or actin (G, H, J). The intensities of the HSP70 bands were determined (one of the gels is shown in H) and are expressed relative to the control (I). Values are mean ± S.E.M. $*P<0.05$; $**P<0.01$; n.s., not significant.
doi:10.1371/journal.pone.0027296.g006

of this study suggest the latter up-regulation is caused by the former down-regulation.

A decrease in the level of HSP70 was also observed in cells treated with 10 μM gefitinib; however, the mechanism governing this decrease seems to be different from that seen with 1 μM gefitinib, because treatment of cells with 10 μM gefitinib caused a decrease in the level of *hsp70* mRNA and in the stability of both *hsp70* mRNA and HSP70. We consider that this high con-

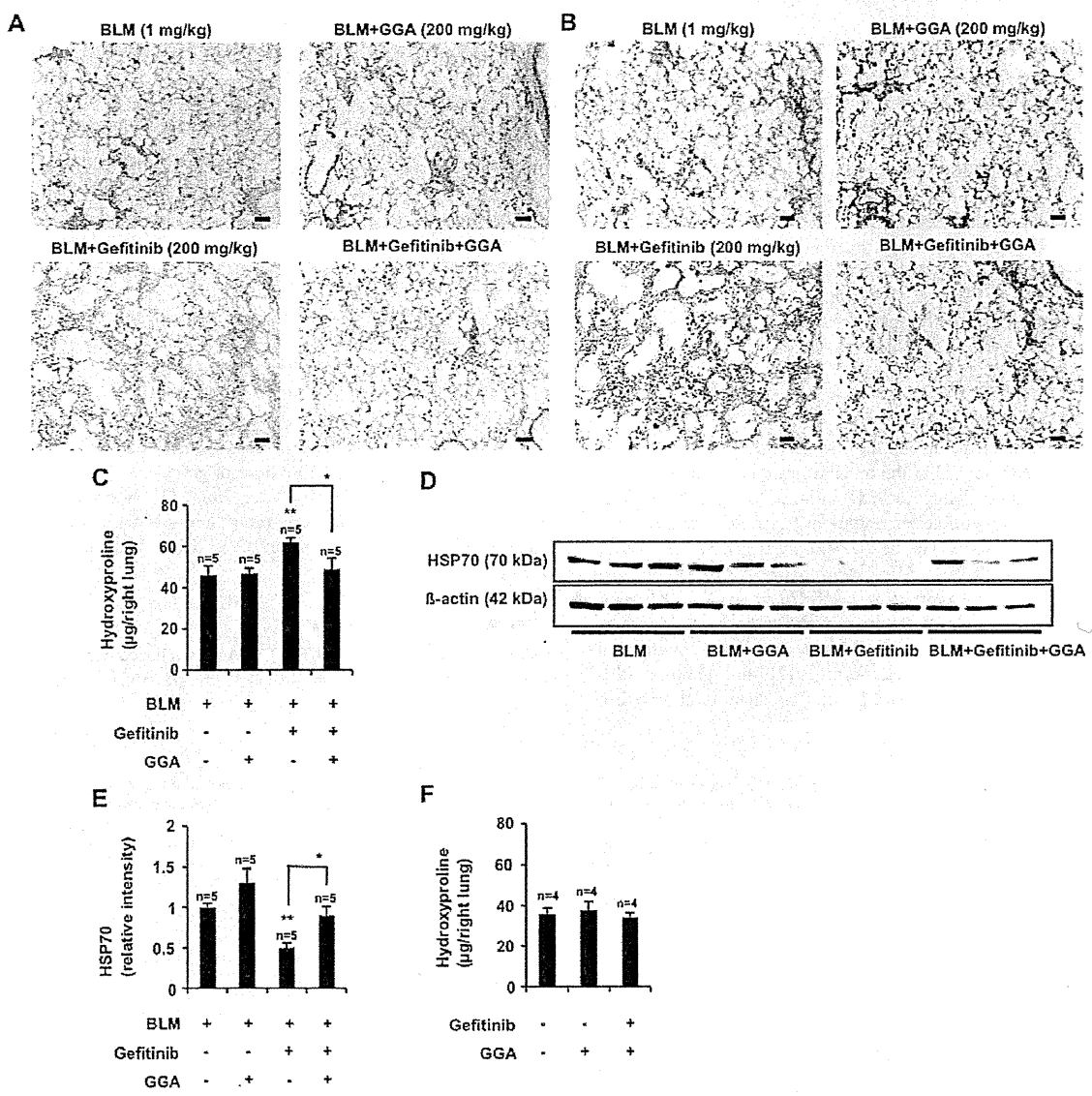

Figure 7. Effect of GGA on gefitinib-dependent exacerbation of pulmonary fibrosis and pulmonary expression of HSP70. Wild-type mice were orally administered gefitinib (200 mg/kg) and/or GGA (200 mg/kg) once per day for 3 days (from day 0 to day 2), then treated once only with 1 mg/kg bleomycin (BLM) (day 3). Mice were then orally administered gefitinib (200 mg/kg) and/or GGA (200 mg/kg) once per 2 days for 14 days (from day 3 to day 17). Sections of pulmonary tissue were prepared at day 17 and subjected to histological examination (H & E staining (A) or Masson's trichrome staining (B)) (scale bar, 50 μm). The pulmonary hydroxyproline levels were determined at day 17 (C). Total protein was extracted from pulmonary tissues at day 17 and analyzed and expressed as described in the legend of Fig. 6 (D, E). Values are mean ± S.E.M. $**P<0.01$; $*P<0.05$.
doi:10.1371/journal.pone.0027296.g007

centration of gefitinib pleiotropically affects various cellular reactions.

After binding EGF, the EGFR is self-phosphorylated and transduces the signal via various mechanisms, including the activation of JNK. Here, we have found that mutations in the EGFR that alter the concentration of gefitinib required for inhibition of EGFR self-phosphorylation affect the gefitinib-dependent decrease in the level of HSP70. Furthermore, an inhibitor of JNK caused a decrease in the level of HSP70. These results suggest that inhibition of EGFR self-phosphorylation and the resulting inhibition of JNK are involved in the gefitinib-dependent decrease in the level of HSP70. However, the manner by which inhibition of JNK suppresses translation of HSP70 remains unclear.

Administration of gefitinib alone did not produce pulmonary fibrosis under our experimental conditions. As one of the risk factors for gefitinib-induced ILD is pre-existing pulmonary fibrosis, we hypothesized that gefitinib stimulates pulmonary fibrosis in the presence of other fibrosis-inducing stimuli. In fact, we found that administration of gefitinib stimulates bleomycin-induced pulmonary fibrosis. Interestingly, this gefitinib-dependent stimulation was not observed so clearly in transgenic mice expressing HSP70, suggesting that expression of HSP70 is involved in the gefitinib-induced exacerbation of bleomycin-induced pulmonary fibrosis. We found that administration of gefitinib suppressed the pulmonary expression of HSP70 and that this suppression was not observed in the transgenic mice expressing HSP70. Taken together, our findings suggest that gefitinib exacerbates bleomycin-induced pulmonary fibrosis through the suppression of HSP70 expression. This finding is an important step towards elucidating the molecular mechanism of drug-induced ILD, as well as the mechanism governing the ethnic differences in susceptibility to ILD induced by the drug. It is possible that the susceptible phenotype of Japanese patients is due to a specific polymorphism in the *hsp70* and *hsf1* genes and in other genes related to HSP70. Also, examination of the effect of candidate drugs on the expression of HSP70 *in vitro* could be used for screening to eliminate those drugs with the potential to induce ILD. Furthermore, exacerbation of bleomycin-induced pulmonary fibrosis was observed with leflunomide [7] and gefitinib (this study), suggesting this model can be used as an animal model of drug-induced pulmonary fibrosis and for screening to eliminate candidate drugs with the potential to induce ILD.

As described above, it was recently reported that administration of GGA ameliorates bleomycin-induced pulmonary fibrosis [51], a result that we confirmed in a previous paper [35], In this study, we found that administration of GGA suppresses the gefitinib-dependent exacerbation of bleomycin-induced pulmonary fibrosis. We consider that this suppression is due to the recovery of HSP70 expression in the lung. As described in the Introduction, a treatment for drug-induced ILD has not been established. We believe that GGA could be beneficial for the treatment of gefitinib-induced ILD, given that the safety of GGA has already been shown clinically.

Supporting Information

Figure S1 Effects of drugs known to induce ILD clinically on expression of HSP70. A549 cells were incubated with the indicated concentration of A771726, amiodarone (AMD), gefitinib or imatinib for 24 h. Whole cell extracts were analyzed by immunoblotting with an antibody against HSP70 or β-actin.
(TIFF)

Figure S2 Time course profile for gefitinib-dependent suppression of expression of HSP70 *in vivo*. Mice were orally administered gefitinib (200 mg/kg) or vehicle once per day for the indicated periods. Total protein was extracted from pulmonary tissues and protein expression was monitored by immunoblotting with an antibody against HSP70 or β-actin.
(TIFF)

Figure S3 Effect of low dose of gefitinib on bleomycin-induced pulmonary fibrosis and pulmonary expression of HSP70. The effect of a low dose of gefitinib (100 mg/kg) on the expression of HSP70 in the lung (A) and pulmonary hydroxyproline levels (B) were monitored as described in the legend of Fig. 6. Values are mean ± S.E.M.
(TIFF)

Author Contributions

Performed the experiments: TN TH TM. Analyzed the data: TN KT TM. Contributed reagents/materials/analysis tools: TN AA TM. Wrote the paper: TN TM.

References

1. Olson AL, Swigris JJ, Lezotte DC, Norris JM, Wilson CG, et al. (2007) Mortality from pulmonary fibrosis increased in the United States from 1992 to 2003. Am J Respir Crit Care Med 176: 277–284.
2. Fumeaux T, Rothmeier C, Jolliet P (2001) Outcome of mechanical ventilation for acute respiratory failure in patients with pulmonary fibrosis. Intensive Care Med 27: 1868–1874.
3. Camus P, Fanton A, Bonniaud P, Camus C, Foucher P (2004) Interstitial lung disease induced by drugs and radiation. Respiration 71: 301–326.
4. Inoue A, Saijo Y, Maemondo M, Gomi K, Tokue Y, et al. (2003) Severe acute interstitial pneumonia and gefitinib. Lancet 361: 137–139.
5. Flieder DB, Travis WD (2004) Pathologic characteristics of drug-induced lung disease. Clin Chest Med 25: 37–45.
6. Moore BB, Hogaboam CM (2008) Murine models of pulmonary fibrosis. Am J Physiol Lung Cell Mol Physiol 294: L152–160.
7. Namba T, Tanaka KI, Ito Y, Hoshino T, Matoyama M, et al. (2010) Induction of EMT-like phenotypes by an active metabolite of leflunomide and its contribution to pulmonary fibrosis. Cell Death Differ 17: 1882–1895.
8. Sheppard D (2006) Transforming growth factor beta: a central modulator of pulmonary and airway inflammation and fibrosis. Proc Am Thorac Soc 3: 413–417.
9. Hinz B, Phan SH, Thannickal VJ, Galli A, Bochaton-Piallat ML, et al. (2007) The myofibroblast: one function, multiple origins. Am J Pathol 170: 1807–1816.
10. Kisseleva T, Brenner DA (2008) Fibrogenesis of parenchymal organs. Proc Am Thorac Soc 5: 338–342.
11. Willis BC, Borok Z (2007) TGF-beta-induced EMT: mechanisms and implications for fibrotic lung disease. Am J Physiol Lung Cell Mol Physiol 293: L525–534.
12. Kasai H, Allen JT, Mason RM, Kamimura T, Zhang Z (2005) TGF-beta1 induces human alveolar epithelial to mesenchymal cell transition (EMT). Respir Res 6: 56.
13. Kim KK, Kugler MC, Wolters PJ, Robillard L, Galvez MG, et al. (2006) Alveolar epithelial cell mesenchymal transition develops in vivo during pulmonary fibrosis and is regulated by the extracellular matrix. Proc Natl Acad Sci U S A 103: 13180–13185.
14. Kim KK, Wei Y, Szekeres C, Kugler MC, Wolters PJ, et al. (2009) Epithelial cell alpha3beta1 integrin links beta-catenin and Smad signaling to promote myofibroblast formation and pulmonary fibrosis. J Clin Invest 119: 213–224.
15. Blackledge G, Averbuch S (2004) Gefitinib ('Iressa', ZD1839) and new epidermal growth factor receptor inhibitors. Br J Cancer 90: 566–572.
16. Lynch TJ, Bell DW, Sordella R, Gurubhagavatula S, Okimoto RA, et al. (2004) Activating mutations in the epidermal growth factor receptor underlying responsiveness of non-small-cell lung cancer to gefitinib. N Engl J Med 350: 2129–2139.
17. Paez JG, Janne PA, Lee JC, Tracy S, Greulich H, et al. (2004) EGFR mutations in lung cancer: correlation with clinical response to gefitinib therapy. Science 304: 1497–1500.
18. Kataoka K, Taniguchi H, Hasegawa Y, Kondoh Y, Kimura T, et al. (2006) Interstitial lung disease associated with gefitinib. Respir Med 100: 698–704.
19. Maemondo M, Inoue A, Kobayashi K, Sugawara S, Oizumi S, et al. (2010) Gefitinib or chemotherapy for non-small-cell lung cancer with mutated EGFR. N Engl J Med 362: 2380–2388.
20. Ando M, Okamoto I, Yamamoto N, Takeda K, Tamura K, et al. (2006) Predictive factors for interstitial lung disease, antitumor response, and survival in

non-small-cell lung cancer patients treated with gefitinib. J Clin Oncol 24: 2549–2556.
21. Kudoh S, Kato H, Nishiwaki Y, Fukuoka M, Nakata K, et al. (2008) Interstitial lung disease in Japanese patients with lung cancer: a cohort and nested case-control study. Am J Respir Crit Care Med 177: 1348–1357.
22. Suzuki H, Aoshiba K, Yokohori N, Nagai A (2003) Epidermal growth factor receptor tyrosine kinase inhibition augments a murine model of pulmonary fibrosis. Cancer Res 63: 5054–5059.
23. Ishii Y, Fujimoto S, Fukuda T (2006) Gefitinib prevents bleomycin-induced lung fibrosis in mice. Am J Respir Crit Care Med 174: 550–556.
24. Richter K, Haslbeck M, Buchner J (2010) The heat shock response: life on the verge of death. Mol Cell 40: 253–266.
25. Mathew A, Morimoto RI (1998) Role of the heat-shock response in the life and death of proteins. Ann N Y Acad Sci 851: 99–111.
26. Hirakawa T, Rokutan K, Nikawa T, Kishi K (1996) Geranylgeranylacetone induces heat shock proteins in cultured guinea pig gastric mucosal cells and rat gastric mucosa. Gastroenterology 111: 345–357.
27. Tomisato W, Takahashi N, Komoto C, Rokutan K, Tsuchiya T, et al. (2000) Geranylgeranylacetone protects cultured guinea pig gastric mucosal cells from indomethacin. Dig Dis Sci 45: 1674–1679.
28. Tang D, Kang R, Xiao W, Wang H, Calderwood SK, et al. (2007) The anti-inflammatory effects of heat shock protein 72 involve inhibition of high-mobility-group box 1 release and proinflammatory function in macrophages. J Immunol 179: 1236–1244.
29. Suemasu S, Tanaka K, Namba T, Ishihara T, Katsu T, et al. (2009) A role for HSP70 in protecting against indomethacin-induced gastric lesions. J Biol Chem 284: 19705–19715.
30. Matsuda M, Hoshino T, Yamashita Y, Tanaka K, Maji D, et al. (2010) Prevention of UVB radiation-induced epidermal damage by expression of heat shock protein 70. J Biol Chem 285: 5848–5858.
31. Tanaka K, Tsutsumi S, Arai Y, Hoshino T, Suzuki K, et al. (2007) Genetic evidence for a protective role of heat shock factor 1 against irritant-induced gastric lesions. Mol Pharmacol 71: 985–993.
32. Tanaka K, Namba T, Arai Y, Fujimoto M, Adachi H, et al. (2007) Genetic Evidence for a Protective Role for Heat Shock Factor 1 and Heat Shock Protein 70 against Colitis. J Biol Chem 282: 23240–23252.
33. Asano T, Tanaka K, Yamakawa N, Adachi H, Sobue G, et al. (2009) HSP70 confers protection against indomethacin-induced lesions of the small intestine. J Pharmacol Exp Ther 330: 458–467.
34. Hoshino T, Murao N, Namba T, Takehara M, Adachi H, et al. (2011) Suppression of Alzheimer's disease-related phenotypes by expression of heat shock protein 70 in mice. J Neurosci 31: 5225–5234.
35. Tanaka K, Tanaka Y, Namba T, Azuma A, Mizushima T (2010) Heat shock protein 70 protects against bleomycin-induced pulmonary fibrosis in mice. Biochem Pharmacol 80: 920–931.
36. Kim VN (2005) MicroRNA biogenesis: coordinated cropping and dicing. Nat Rev Mol Cell Biol 6: 376–385.
37. Liu G, Friggeri A, Yang Y, Milosevic J, Ding Q, et al. (2010) miR-21 mediates fibrogenic activation of pulmonary fibroblasts and lung fibrosis. J Exp Med 207: 1589–1597.
38. Namba T, Homan T, Nishimura T, Mima S, Hoshino T, et al. (2009) Up-regulation of S100P expression by non-steroidal anti-inflammatory drugs and its role in anti-tumorigenic effects. J Biol Chem 284: 4158–4167.
39. Bradford MM (1976) A rapid and sensitive method for the quantitation of microgram quantities of protein utilizing the principle of protein-dye binding. Anal Biochem 72: 248–254.
40. Chu CY, Rana TM (2006) Translation repression in human cells by microRNA-induced gene silencing requires RCK/p54. PLoS Biol 4: e210.
41. Tanaka K, Ishihara T, Azuma A, Kudoh S, Ebina M, et al. (2010) Therapeutic effect of lecithinized superoxide dismutase on bleomycin-induced pulmonary fibrosis. Am J Physiol Lung Cell Mol Physiol 298: L348–360.
42. Gridelli C, Bareschino MA, Schettino C, Rossi A, Maione P, et al. (2007) Erlotinib in non-small cell lung cancer treatment: current status and future development. Oncologist 12: 840–849.
43. Ono M, Hirata A, Kometani T, Miyagawa M, Ueda S, et al. (2004) Sensitivity to gefitinib (Iressa, ZD1839) in non-small cell lung cancer cell lines correlates with dependence on the epidermal growth factor (EGF) receptor/extracellular signal-regulated kinase 1/2 and EGF receptor/Akt pathway for proliferation. Mol Cancer Ther 3: 465–472.
44. Van Schaeybroeck S, Kyula J, Kelly DM, Karaiskou-McCaul A, Stokesberry SA, et al. (2006) Chemotherapy-induced epidermal growth factor receptor activation determines response to combined gefitinib/chemotherapy treatment in non-small cell lung cancer cells. Mol Cancer Ther 5: 1154–1165.
45. Miyata H, Sasaki T, Kuwahara K, Serikawa M, Chayama K (2006) The effects of ZD1839 (Iressa), a highly selective EGFR tyrosine kinase inhibitor, as a radiosensitiser in bile duct carcinoma cell lines. Int J Oncol 28: 915–921.
46. Moon DO, Kim MO, Lee JD, Choi YH, Lee MK, et al. (2007) Molecular mechanisms of ZD1839 (Iressa)-induced apoptosis in human leukemic U937 cells. Acta Pharmacol Sin 28: 1205–1214.
47. Li J, Karlsson MO, Brahmer J, Spitz A, Zhao M, et al. (2006) CYP3A phenotyping approach to predict systemic exposure to EGFR tyrosine kinase inhibitors. J Natl Cancer Inst 98: 1714–1723.
48. Li Y, Vandenboom TG, 2nd, Wang Z, Kong D, Ali S, et al. (2010) miR-146a suppresses invasion of pancreatic cancer cells. Cancer Res 70: 1486–1495.
49. Hurst DR, Edmonds MD, Scott GK, Benz CC, Vaidya KS, et al. (2009) Breast cancer metastasis suppressor 1 up-regulates miR-146, which suppresses breast cancer metastasis. Cancer Res 69: 1279–1283.
50. Leu JI, Pimkina J, Frank A, Murphy ME, George DL (2009) A small molecule inhibitor of inducible heat shock protein 70. Mol Cell 36: 15–27.
51. Fujibayashi T, Hashimoto N, Jijiwa M, Hasegawa Y, Kojima T, et al. (2009) Protective effect of geranylgeranylacetone, an inducer of heat shock protein 70, against drug-induced lung injury/fibrosis in an animal model. BMC Pulm Med 9: 45.

Journal of Neurochemistry JNC

JOURNAL OF NEUROCHEMISTRY | 2012 | 120 | 795–805 doi: 10.1111/j.1471-4159.2011.07567.x

ORIGINAL ARTICLE

Improvement of cognitive function in Alzheimer's disease model mice by genetic and pharmacological inhibition of the EP_4 receptor

Tatsuya Hoshino,*,† Takushi Namba,† Masaya Takehara,† Naoya Murao,† Takahide Matsushima,‡ Yukihiko Sugimoto,† Shuh Narumiya,§ Toshiharu Suzuki‡ and Tohru Mizushima*,†

*Faculty of Pharmacy, Keio University, Tokyo, Japan

†Graduate School of Medical and Pharmaceutical Sciences, Kumamoto University, Kumamoto, Japan

‡Graduate School of Pharmaceutical Sciences, Hokkaido University, Sapporo, Japan

§Faculty of Medicine, Kyoto University, Kyoto, Japan

Abstract

Amyloid-β peptide (Aβ), which is generated by the β- and γ-secretase-mediated proteolysis of β-amyloid precursor protein (APP), plays an important role in the pathogenesis of Alzheimer's disease (AD). We recently reported that prostaglandin E_2 (PGE_2) stimulates the production of Aβ through both EP_2 and EP_4 receptors and that activation of the EP_4 receptor stimulates Aβ production through endocytosis and activation of γ-secretase. We here found that transgenic mice expressing mutant APP (APP23) mice showed a greater or lesser apparent cognitive deficit when they were crossed with mice lacking EP_2 or EP_4 receptors, respectively. Mice lacking the EP_4 receptor also displayed lower levels of Aβ plaque deposition and less neuronal and synaptic loss than control mice. Oral administration of a specific EP_4 receptor antagonist, AE3-208 to APP23 mice, improved their cognitive performance, as well as decreasing brain levels of Aβ and suppressing endocytosis and activation of γ-secretase. Taken together, these results suggest that inhibition of the EP_4 receptor improves the cognitive function of APP23 mice by suppressing Aβ production and reducing neuronal and synaptic loss. We therefore propose that EP_4 receptor antagonists, such as AE3-208, could be therapeutically beneficial for the prevention and treatment of AD.

Keywords: Alzheimer disease, aging, infammation, memory, neurodegeneration.

J. Neurochem. (2012) **120**, 795–805.

Alzheimer's disease (AD) is the most common neurodegenerative disorder of the central nervous system and the leading cause of adult onset dementia, affecting 5% of the population over the age of 65. Pathological characters of AD are accumulation of neurofibrillary tangles and senile plaques and senile plaques are composed of amyloid-β peptides (Aβ), such as Aβ40 and Aβ42 (Mattson 2004). In order to generate Aβ, β-amyloid precursor protein (APP) is first cleaved by β-secretase and then by γ-secretase (Sisodia and St George-Hyslop 2002). Monomeric Aβ easily self-assembles to form oligomers and protofibrils, which play an important role in the induction of the neuronal and synaptic loss that results in cognitive decline (Haass and Selkoe 2007). γ-Secretase is composed of four core components, including presenilin (PS)-1 and PS-2 (Haass 2004). Early onset familial AD is linked to three genes, *app*, *ps1* and *ps2* (Haass 2004), strongly suggesting that Aβ is a key factor in the pathogenesis of AD. Consequently, cellular factors that affect the production of Aβ represent good targets for drugs to prevent or treat AD.

It has been suggested that inflammation is important in the pathogenesis of AD; chronic inflammation has been observed

Received July 28, 2011; revised manuscript received October 28, 2011; accepted October 28, 2011.

Address correspondence and reprint requests to Tohru Mizushima, Faculty of Pharmacy, Keio University, 1-5-30 Shibakoen, Minato-ku, Tokyo 105-8512, Japan. E-mail: mizushima-th@pha.keio.ac.jp

Abbreviations used: Aβ, amyloid-β peptide; AD, Alzheimer's disease; APP, β-amyloid precursor protein; COX, cyclooxygenase; CTF, C-terminal fragment; LTP, long-term potentiation; NeuN, neuronal nuclei; NSAIDs, non-steroidal anti-inflammatory drugs; PGE_2, prostaglandin E_2; PKA, protein kinase A; PS, presenilin.

in the brains of AD patients, and trauma to the brain and ischemia, both of which can activate inflammation, are major risk factors for the disease (Ikonomovic *et al.* 2004; Wyss-Coray 2006). Cyclooxygenase (COX), which exists as two subtypes, COX-1 and COX-2, is essential for the synthesis of prostaglandin E_2 (PGE_2), a potent inducer of inflammation. COX-1 is expressed constitutively, whereas COX-2 expression is induced under inflammatory conditions and is responsible for the progression of inflammation (Srinivasan and Kulkarni 1989; Smith *et al.* 1998). It has been suggested that the COX-2-mediated production of PGE_2 plays an important role in the pathogenesis of AD. For example, elevated levels of PGE_2 and over-expression of COX-2 have been observed in AD patient brains (Kitamura *et al.* 1999; Montine *et al.* 1999); the extent of COX-2 expression correlates with the degree of progression of AD pathogenesis (Ho *et al.* 2001); transgenic mice constitutively over-expressing COX-2 show aging-dependent memory dysfunction (Andreasson *et al.* 2001); PGE_2 stimulates the production of reactive oxygen species in microglia and activates β-secretase (Liang *et al.* 2005); and prolonged use of non-steroidal anti-inflammatory drugs (NSAIDs), inhibitors of COX, delays the onset and reduces the risk of AD (in t' Veld *et al.* 2001; Imbimbo *et al.* 2010). Thus, in order to identify molecular targets for the development of AD drugs, it is important to understand the molecular mechanism involved in the PGE_2-mediated progression of the disease.

We recently reported that PGE_2 stimulates the production of Aβ in cells stably expressing a form of APP with two mutations (K651N/M652L; APPsw) that elevates cellular and secreted levels of Aβ (Hoshino *et al.* 2007). Using agonists and antagonists specific for each of the four PGE_2 receptors (EP_1, EP_2, EP_3 and EP_4 receptors), we found that both EP_2 and EP_4 receptors are involved in the PGE_2-stimulated production of Aβ *in vitro* (Hoshino *et al.* 2007). With respect to the mechanism underpinning this stimulation, we also recently demonstrated that activation of the EP_2 receptor stimulates the production of Aβ through activation of adenylate cyclase, an increase in the cellular level of cAMP and activation of protein kinase A (PKA) (Hoshino *et al.* 2009). In contrast, EP_4 receptor activation causes its co-internalization with PS-1 (γ-secretase) into endosomes, a process that activates γ-secretase (Hoshino *et al.* 2009). Furthermore, we showed that deletion of the EP_2 or EP_4 receptor decreases brain levels of Aβ in transgenic mice expressing APPsw (APP23, a mouse model for AD), suggesting that EP_2 or EP_4 receptor activation stimulates the production of Aβ *in vivo* (Hoshino *et al.* 2007). These previous results suggest that EP_2 and/or EP_4 receptors could represent valuable molecular targets for the treatment of AD. However, the effect of deletion of these receptors on other AD-related phenotypes, such as neuronal and synaptic loss and cognitive deficits, has not been tested. The effect on cognitive performance is particularly important, because functional phenotypes (cognitive dysfunction) and pathological phenotypes (such as an increase in the brain level of Aβ) are not always directly linked (Roberson *et al.* 2007; Kanninen *et al.* 2009). In this study, we therefore examined the effect of EP_2 and EP_4 receptor inhibition on cognitive function in APP23 mice, revealing that genetic inhibition of the EP_4 receptor but not the EP_2 receptor not only suppresses neuronal and synaptic loss but also improves cognitive performance. Similarly, oral administration of AE3-208, an EP_4 receptor-specific antagonist, improved the cognitive function of the APP23 mice. These results suggest that the EP_4 receptor is a valuable molecular target for the development of drugs to prevent or treat AD.

Materials and methods

Materials and animals

See Appendix S1.

Morris water maze test

The Morris water maze test was conducted in a circular 90- or 150-cm diameter pool filled with water at a temperature of 22.0 + 1°C, as described previously (Kobayashi *et al.* 2000; Huang *et al.* 2006), with some minor modifications. Details are described in Appendix S1.

ELISA for Aβ and β- and γ-secretase-mediated peptide cleavage assay

Aβ40 and Aβ42 levels and β- and γ-secretase activity in the brain were determined as described previously (Hoshino *et al.* 2007). Details are described in Appendix S1.

Thioflavin-S staining and immunohistochemical and immunofluorescence analyses

Thioflavin-S staining and immunohistochemical and immunofluorescence analyses were performed as detailed in Appendix S1.

Statistical analysis

All values are expressed as the mean ± standard error of the mean (SEM). One- or two-way ANOVA followed by the Tukey test was used to evaluate differences between more than two groups. The Student's *t*-test for unpaired results was used for the evaluation of differences between two groups. Differences were considered to be significant for values of $p < 0.05$.

Results

Effect of deletion of EP_2 or EP_4 receptor on cognitive function in APP23 mice

We first used a Morris water maze to compare the spatial learning and memory of 6-month-old APPsw/EP_2−/− and APPsw/EP_4−/− mice with that of APPsw/EP_2+/+ and APPsw/EP_4+/+ mice, respectively. Mice were trained for 7 days to learn the location of a hidden platform, and the time required to reach the platform (escape latency) was

measured. As shown Fig. 1(a), APPsw/EP_2−/− mice required a longer time than APPsw/EP_2+/+ animals to reach the platform, suggesting that EP_2 receptor deletion exacerbates the cognitive deficit in the APP23 mice. In contrast, the APPsw/EP_4−/− mice tended to take less time to reach the platform than the corresponding control animals (APPsw/EP_4+/+) (Fig. 1b), suggesting that deletion of the EP_4 receptor ameliorates the cognitive deficit. These differences did not reflect differences in swimming ability, because swimming speed and the ability to locate a visible platform were similar between the groups (data not shown).

Given that the above results suggest that the EP_4 receptor may represent the better potential molecular target for the development of AD drugs, we next compared AD-related phenotypes, such as the formation of plaques and neuronal and synaptic loss, between four strains of mice (WT/EP_4+/+, WT/EP_4−/−, APPsw/EP_4+/+ and APPsw/EP_4−/−). We first repeated the Morris water maze test using 6-month-old mice, under slightly different experimental conditions (such as the size of swimming pool and tracking period). As shown Fig. 2(a), APPsw/EP_4+/+ mice required a longer time than WT/EP_4+/+ mice to reach the platform and this result is consistent with previous reports (Van Dam *et al.* 2003). Again, this difference did not reflect reduced swimming ability, as the swimming speed and the ability to locate a visible platform were similar between the four strains (data not shown). APPsw/EP_4−/− mice required a shorter time to reach the platform than APPsw/EP_4+/+ mice (Fig. 2a). Furthermore, there was no significant difference in the escape latency between APPsw/EP_4−/− and WT/EP_4+/+

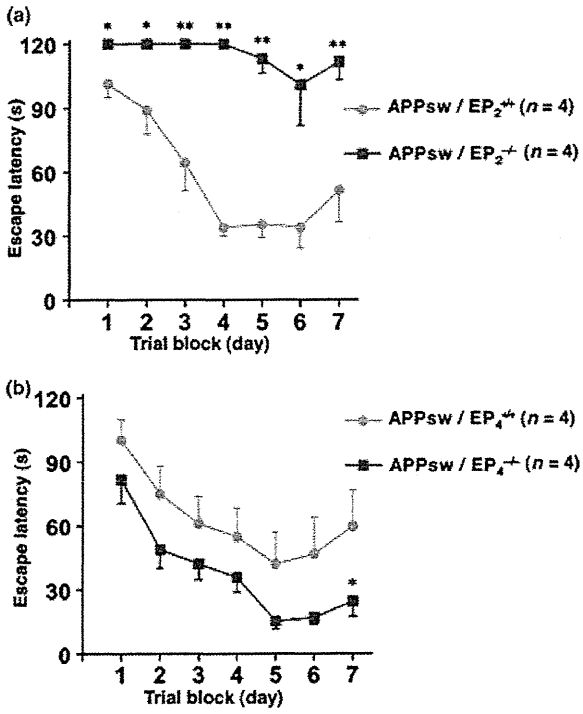

Fig. 1 Effects of deletion of the EP_2 or EP_4 receptor on spatial learning and memory in APP23 mice. Cognitive behavioral tests were carried out, using the Morris water maze, on 6-month-old APPsw/EP_2+/+ and APPsw/EP_2−/− (a) or APPsw/EP_4+/+ and APPsw/EP_4−/− (b) mice as described in the Materials and methods. Swimming paths in a circular 150-cm diameter pool were tracked for 120 s and the average (four tests) escape latency in each trial block was determined for 7 days. Values are given as mean ± SEM. Student's *t*-test: $^{**}p < 0.01$ and $^{*}p < 0.05$.

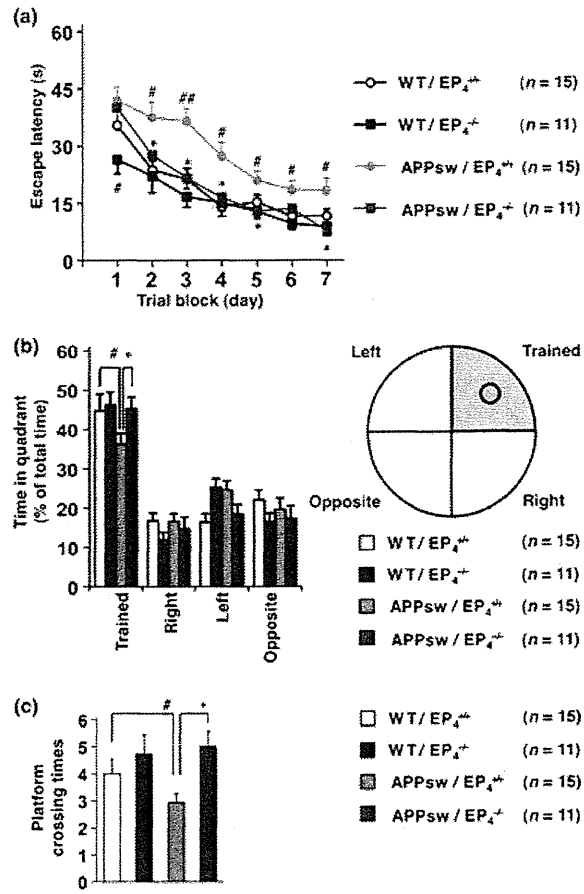

Fig. 2 Effects of deletion of the EP_4 receptor on spatial learning and memory in APP23 mice. Cognitive behavioral tests were carried out on 6-month-old WT/EP_4+/+, WT/EP_4−/−, APPsw/EP_4+/+ and APPsw/EP_4−/− mice. The swimming path in a circular 90-cm diameter pool was tracked for 60 s (a). Mice were subjected to a transfer test in which the platform was removed. The spatial memory for a platform location was estimated by per cent search time in each quadrant (the platform had been located in the 'trained' quadrant) (b) or platform crossing times (c). Values are given as mean ± SEM. One-way (b, c) or two-way (a) ANOVA followed by Tukey test: $^{*}p < 0.05$, versus APPsw/ EP_4+/+ mice; $^{\#\#}p < 0.01$ and $^{\#}p < 0.05$, versus WT/ EP_4+/+ mice.

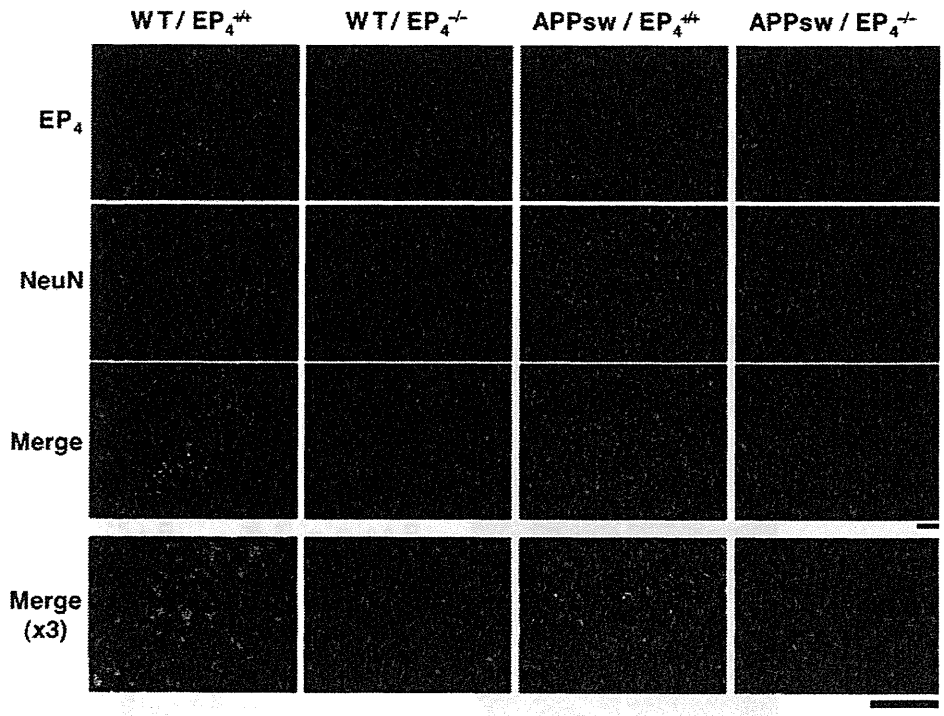

Fig. 3 EP_4 receptor expression in hippocampal neurons. Brain sections from 18-month-old WT/EP_4+/+, WT/EP_4−/−, APPsw/EP_4+/+ and APPsw/EP_4−/− mice were immunohistochemically labeled by immunofluorescence technique with antibodies against the EP_4 receptor and NeuN. The hippocampal CA3 region is shown (scale bar, 100 μm).

mice (Fig. 2a). These results suggest that the expression of APPsw disturbs spatial learning and memory and this effect can be ameliorated by deletion of the EP_4 receptor. WT/EP_4−/− mice took a significantly shorter time to reach the platform than WT/EP_4+/+ mice; however, the difference was observed only at day 0 (Fig. 2a).

We then did a transfer test to examine the spatial memory of platform location. After a 7-day training period as described above, each mouse was subjected to a Morris water maze test where the platform was removed and we measured the per cent search time for each quadrant. As shown in Fig. 2(b), the percentage of time spent in the trained quadrant was lower for the APPsw/EP_4+/+ group than for either the WT/EP_4+/+ or the APPsw/EP_4−/− mice. The crossing time of the area where the platform had been located was lower in the APPsw/EP_4+/+ group than in the WT/EP_4+/+ and APPsw/EP_4−/− cohorts (Fig. 2c). There was no significant difference between APPsw/EP_4−/− and WT/EP_4+/+ mice or between WT/EP_4−/− and WT/ EP_4+/+ mice for these indices (Fig. 2b and c). These results showed that deletion of the EP_4 receptor ameliorates the spatial memory deficits of APP23 mice.

We then examined EP_4 receptor expression in the brain of 18-month-old mice (hippocampal CA3 region) by immunofluorescence analysis. As shown in Fig. 3, expression of the receptor was clearly observed in the brains of WT/EP_4+/+ and APPsw/EP_4+/+ mice. Staining with antibody against neuronal nuclei (NeuN) confirmed expression of the EP_4 receptor in neurons (Fig. 3), consistent with previous results (Choi *et al.* 2006). However, co-staining with antibody against NeuN and that against glial fibrillary acidic protein (a maker for astrocytes) or F4/80 (a maker for microglia) was not so clear (Fig. S1).

Effect of deletion of EP_4 receptor on Aβ plaque deposition and neuronal and synaptic loss in APP23 mice

We have previously reported that the levels of Aβ40 and Aβ42 in soluble and insoluble brain fractions prepared from 6-month-old APPsw/EP_4−/− mice are lower than those from APPsw/EP_4+/+ mice (Hoshino *et al.* 2007), a finding that we confirmed here (Fig. 4a). We also examined Aβ plaque deposition by thioflavin-S staining using 18-month-old mice. As shown in Fig. 4(b) and (c), in both the hippocampus and the cerebral cortex, the level of Aβ plaque deposition was much lower in APPsw/EP_4−/− mice than in APPsw/EP_4+/+ animals.

We next determined the number of neurons in the hippocampal CA3 region by NeuN staining using 18-month-old mice. As shown in Fig. 4(d) and (e), the number of NeuN-positive cells (neurons) was significantly

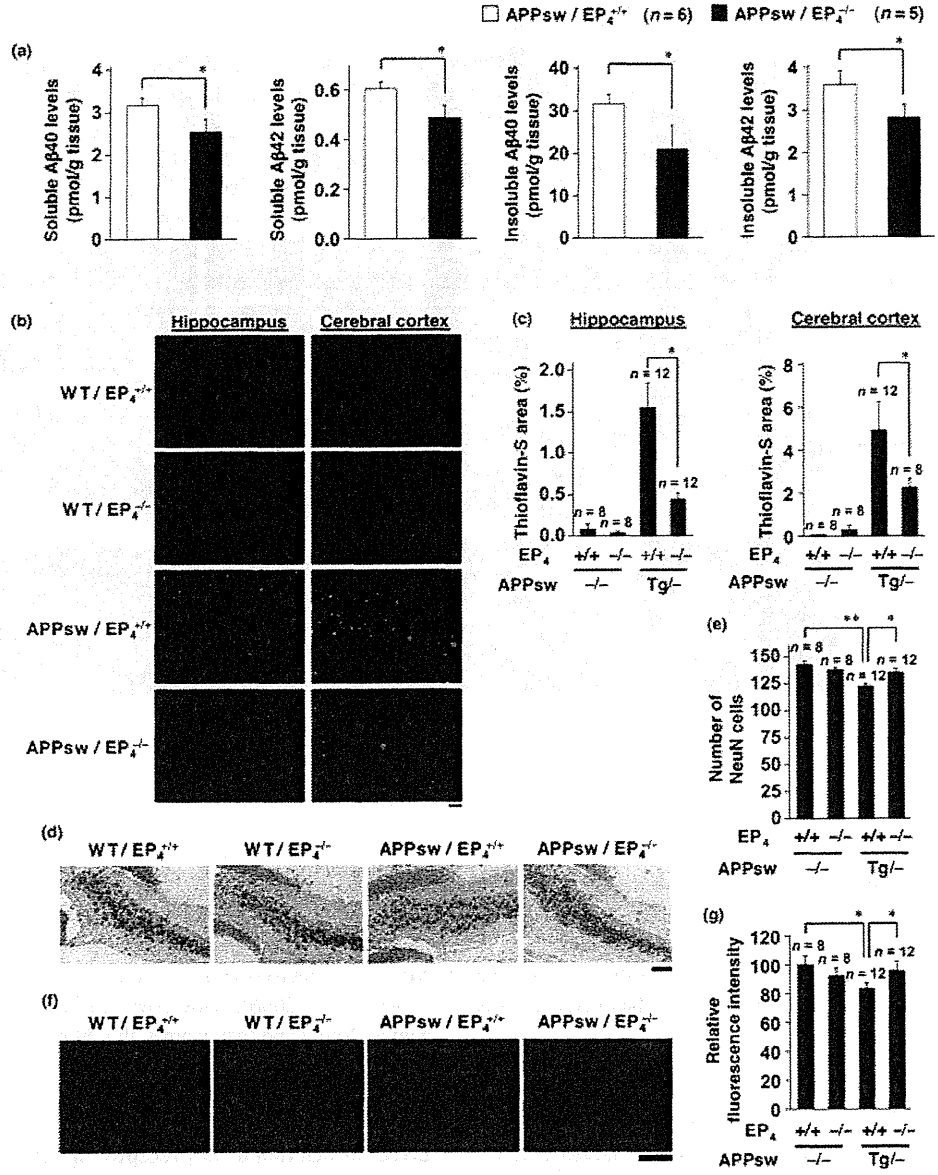

Fig. 4 Effects of EP_4 receptor deletion on Aβ levels, Aβ plaque deposition and neuronal and synaptic loss in APP23 mice. Soluble and insoluble fractions were prepared from the brains of 6-month-old APPsw/EP_4+/+ and APPsw/EP_4−/− mice. The amounts of Aβ40 and Aβ42 in each fraction were determined by ELISA as described in the Materials and methods (a). Values are given as mean ± SEM. Student's *t*-test: $^*p < 0.05$. Brain sections from 18-month-old APPsw/EP_4+/+, APPsw/EP_4−/−, WT/EP_4+/+ and WT/ EP_4−/− mice were applied to thioflavin-S staining (scale bar, 200 μm) (b) or immunohistochemical analysis with an antibody against NeuN (scale bar, 100 μm) (d) or immunofluorescence analysis with an antibody against synaptophysin (scale bar, 50 μm) (f). The relative area positive for thioflavin-S staining (c), the number of NeuN-positive cells in the hippocampal CA3 region (e) and the relative fluorescence intensity in the region (g) were determined (three sections per brain). Values are given as mean ± SEM. One-way ANOVA followed by Tukey test: $^{**}p < 0.01$; $^*p < 0.05$.

higher in the WT/EP_4+/+ and APPsw/EP_4−/− brain sections than in the APPsw/EP_4+/+ tissue, suggesting that the neuronal loss induced by Aβ was ameliorated by deletion of the EP_4 receptor. Similar results were observed for the hippocampal CA1 region (Fig. S2). We also estimated the number of synapses by synaptophysin staining using 18-month-old mice. The level of synaptophysin was higher in sections from both WT/EP_4+/+ and APPsw/EP_4−/− mice

than in those from APPsw/EP_4+/+ mice (Fig. 4f and g), indicating that Aβ-induced synaptic loss was suppressed by deletion of the EP_4 receptor. Taken together, these results suggest that deletion of the EP_4 receptor decreases the level of Aβ and Aβ plaque deposition in the brain and protects against Aβ-induced neurodegeneration. To confirm this further, stereological quantification of cell number that is more reliable should be performed in future studies.

Effect of oral administration of AE3-208 on AD-related phenotypes in APP23 mice

The results described above suggest that pharmacological inhibition of the EP_4 receptor ameliorates AD-related phenotypes in APP23 mice. In order to test this, we used an EP_4 receptor-specific antagonist, AE3-208. The K_i values of AE3-208 obtained by competition binding assay are 1.3, 30, 790 and 2400 nM for EP_4, EP_3, FP and TP, respectively, and more than 10 μM for the other prostanoid receptors (Kabashima *et al.* 2002). We have previously reported that AE3-208 suppresses the PGE_2-stimulated production of Aβ *in vitro* (Hoshino *et al.* 2007). APP23 and wild-type mice were fed either AE3-208-supplemented chow or a control diet between the ages of 3 and 6 months (the average dose of AE3-208 was calculated to be 17.8 mg/kg body weight/day). No significant differences were observed in the amount of chow consumed by the four groups of mice (APP23 or wild-type mice fed AE3-208-supplemented or control chow) during the experimental period. We then examined the spatial learning and memory of the 6-month-old animals in a Morris water maze test. Swimming speed and ability to locate a visible platform were indistinguishable between the four groups (data not shown). However, APP23 mice fed AE3-208-supplemented chow took significantly less time to find the hidden platform than the mice fed control chow (Fig. 5a). No significant difference in the escape latency was recorded between wild-type mice fed AE3-208-supplemented chow and wild-type mice fed control chow (Fig. 5a). These results suggest that the deficit in spatial learning and memory in the APP23 mice can be ameliorated by oral administration of AE3-208.

As shown in Fig. 5(b), the amount of time spent in the trained quadrant showed a tendency to be greater for the APP23 mice fed AE3-208-supplemented chow than for the mice fed control chow. Furthermore, the crossing time of the area where the platform had been located was significantly greater in the former case (Fig. 5c). However, the difference in Fig. 5(b) was not statistically significant and we have no clear explanation for the discrepancy between the 'time in quadrant' and 'platform crossings' outcomes.

In order to test whether pharmacological inhibition of the EP_4 receptor ameliorates AD-related pathological phenotypes in APP23 mice, we compared the amount of Aβ40 and Aβ42 in soluble and insoluble fractions prepared from the brains of APP23 mice fed either AE3-208-supplemented or

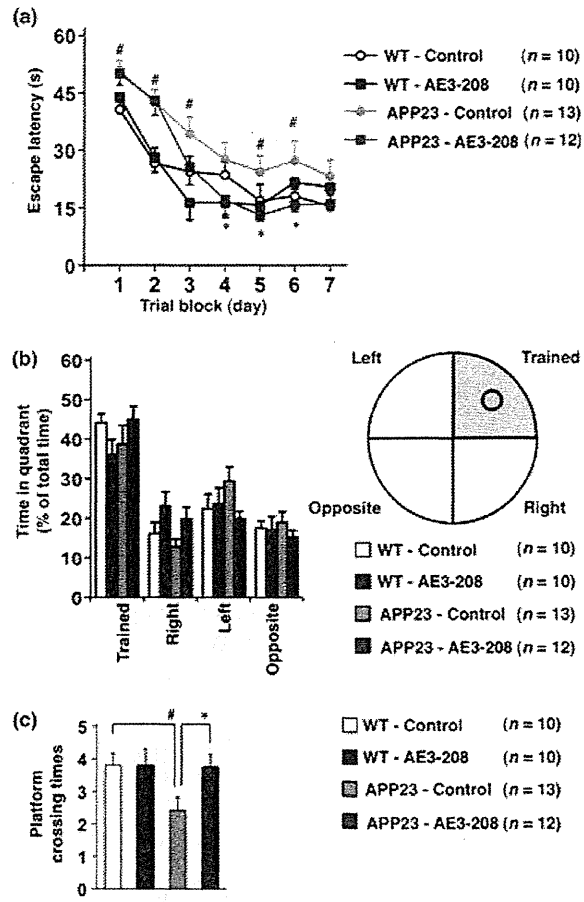

Fig. 5 Effects of oral administration of AE3-208 on spatial learning and memory in APP23 mice. Cognitive behavioral tests were carried out, using the Morris water maze, on 6-month-old wild-type mice (WT) and APP23 mice fed either AE3-208-supplemented chow (160 mg AE3-208/kg chow) or control chow between the ages of 3 and 6 months. Spatial learning and memory were tested as described in the legend of Fig. 2 (a–c). Values are given as mean ± SEM. One-way (b, c) or two-way (a) ANOVA followed by Tukey test: $^*p < 0.05$, versus APP23-control mice; $^\#p < 0.05$, versus WT-control mice.

control chow using 6-month-old mice. As shown in Fig. 6(a), the levels of Aβ40 and Aβ42 in the insoluble brain fractions from the former group were significantly lower. However, no significant difference was observed in the case of the soluble fractions (Fig. 6a).

We have previously reported that EP_4 receptor activation increases Aβ levels through its co-internalization into endosomes with PS-1 (γ-secretase), with resulting activation of γ-secretase *in vitro* (Hoshino *et al.* 2009). This finding was supported by our previous *in vivo* demonstration that brain γ-secretase activity is lower in APPsw/EP_4−/− mice than in APPsw/EP_4+/+ animals, and that the co-localization of PS-1 with Rab7 (a marker of late endosomes and

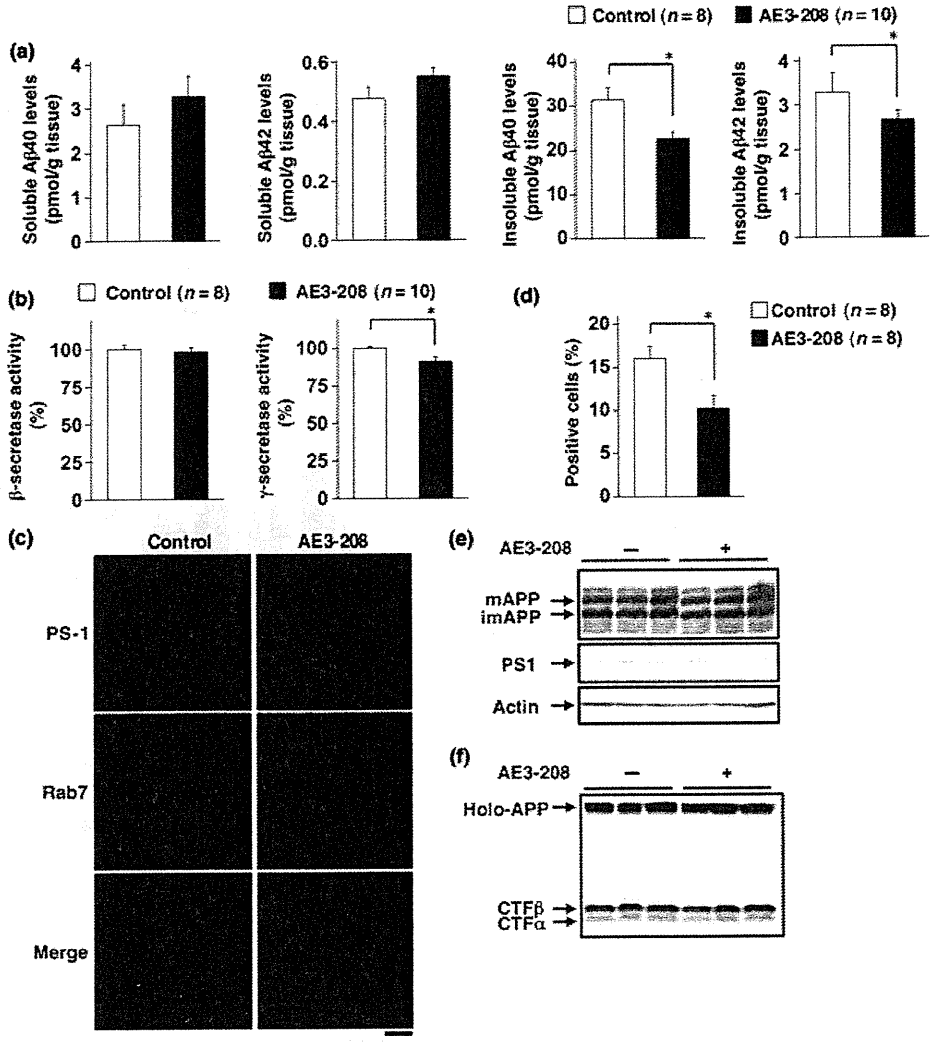

Fig. 6 Effects of oral administration of AE3-208 on Aβ levels, secretase activity, localization of γ-secretase and APP modulation in the APP23 mouse brain. APP23 mice were treated with AE3-208, as described in the legend of Fig. 5 (a–c). (6-month-old) The amounts of Aβ40 and Aβ42 were determined as described in the legend of Fig. 4 (a). Membrane fractions were prepared and subjected to a β- or γ- secretase-mediated peptide cleavage assay as described in the Materials and methods (b). Brain sections were immunostained with antibodies against PS-1 and Rab7 (scale bar, 200 μm) (c). Cells positive for both PS-1 and Rab7 staining were counted (d). Whole-cell extracts were subjected to immunoblotting with an antibody to APP (e, f), PS-1 (e) or actin (e). Values are given as mean ± SEM. Student's *t*-test: $^*p < 0.05$.

lysosomes) is not as apparent in the former group (Hoshino *et al.* 2009). In the present study, we examined the effect of oral administration of AE3-208 on the activity and localization of γ-secretase using 6-month-old mice. As shown in Fig. 6(b), the activity of γ-secretase, but not that of β-secretase, was lower in the brains of APP23 mice fed AE3-208-supplemented chow than in those of mice fed control chow. Furthermore, we found that the co-localization of PS-1 with Rab7 was not as apparent in the former group (Fig. 6c and d). We quantitatively examined the effect of AE3-208 on the expression of PS-1 staining and found that the effect was not statistically significant (data not shown).

We have previously reported that deletion of the EP_4 receptor in APP23 mice does not affect the modification of APP or α- and β-secretase activity (Hoshino *et al.* 2009), both of which are important for Aβ production. Here, we examined the effect of oral administration of AE3-208 on these processes using 6-month-old mice. We could separate by sodium dodecyl sulfate–polyacrylamide gel electrophoresis between the mature (*N*- and *O*-glycosylated) and

immature (*N*-glycosylated alone) forms of APP (mAPP and imAPP, respectively) (Tomita *et al.* 1998). As shown in Fig. 6(e), the total amount of APP and the ratio of mAPP and imAPP were similar between APP23 mice fed AE3-208-supplemented chow and those fed control chow, suggesting that the administration of AE3-208 does not affect APP modulation. We also found that the administration of AE3-208 did not affect the level of PS-1 (Fig. 6e). We then examined α- and β-secretase activity by comparing the level of secreted C-terminal fragment (CTF), representing an indirect index of secretase activity. We could not detect a CTFγ band under our experimental conditions. However, as shown in Fig. 6(f), CTFα and CTFβ were detected in the APP23 mice and the amounts of CTFα and CTFβ were indistinguishable between APP23 mice fed AE3-208-supplemented chow and those fed control chow, thereby suggesting that the administration of AE3-208 does not affect α- or β-secretase activity.

Taken together, these results suggest that the improvement in the cognitive function of the APP23 mice orally administered AE3-208 is mediated by a decrease in the brain levels of Aβ through suppression of co-internalization of the EP_4 receptor with γ-secretase into endosomes, thereby inhibiting the activation of γ-secretase.

Discussion

We have previously suggested that EP_2 and EP_4 receptors represent valuable molecular targets for the development of drugs to prevent or treat AD by showing that the amount of Aβ in the brains of APPsw/EP_2−/− and APPsw/EP_4−/− mice is lower than that in the respective control mice (Hoshino *et al.* 2007). However, among the antagonists specific for either the EP_2 or EP_4 receptor, or both, which type offers the most therapeutic potential? In order to address this issue, we herein compared the cognitive performance of APPsw/EP_2−/− or APPsw/EP_4−/− mice with that of their respective wild-type counterparts. This approach was adopted because, although AD is characterized by cognitive impairment, the functional (cognitive) phenotypes and pathological phenotypes (such as an increase in Aβ levels and Aβ plaque deposition) of the disease are not always directly linked. For example, some conditions ameliorate cognitive dysfunction in AD model mice without affecting the pathological phenotypes (Roberson *et al.* 2007; Kanninen *et al.* 2009). Our results suggested that APPsw/EP_4−/− mice but not APPsw/EP_2−/− mice display a higher level of cognitive function (spatial learning and memory) than their respective wild-type controls, suggesting that inhibition of the EP_4 receptor might prove the better therapeutic option.

We have previously reported that PGE_2-stimulated production of Aβ *in vitro* is partially mediated by EP_2 receptor-dependent activation of the cAMP–PKA pathway (Hoshino *et al.* 2009), and that the amount of Aβ in the brains of APPsw/EP_2−/− mice is lower than that in control mice (Hoshino *et al.* 2007). Another group has also shown that deletion of the EP_2 receptor in AD model mice reduces Aβ plaque deposition (Liang *et al.* 2005). Thus, it is surprising that deletion of this receptor exacerbates cognitive dysfunction in APP23 mice, suggesting that deletion of the EP_2 receptor impaired cognitive performance through an Aβ-independent mechanism. It has previously been reported that Aβ inhibits long-term potentiation (LTP) through inhibition of the cAMP–PKA pathway (Vitolo *et al.* 2002), and that inhibition of the EP_2 receptor also suppresses LTP via a similar mechanism (Akaneya and Tsumoto 2006). Thus, deletion of the EP_2 receptor may exacerbate cognitive dysfunction in APP23 mice through inhibition of LTP, a process known to be important for memory formation. It was recently reported that deletion of the gene encoding EP_2 receptor in mice without the expression of APPsw have behavioral deficits (Savonenko *et al.* 2009), thus it is unclear whether the observed effects of EP_2 receptor deletion in this study are specific to the AD model. However, it was previously reported that siRNA for EP_4 did not affect LTP (Akaneya and Tsumoto 2006).

We have previously reported that EP_4 receptor activation stimulates the production of Aβ through its co-internalization with γ-secretase into endosomes, leading to the activation of γ-secretase (Hoshino *et al.* 2009). We also showed that there are lower levels of Aβ and less endosomal localization of γ-secretase in the brains of APPsw/EP_4−/− mice than in those of APPsw/EP_4+/+ animals (Hoshino *et al.* 2007, 2009). Furthermore, in the present study, we have demonstrated that APPsw/EP_4−/− mice display lower levels of Aβ plaque formation and neuronal and synaptic loss than APPsw/EP_4+/+ mice. These results suggest that deletion of the EP_4 receptor ameliorates cognitive dysfunction in APP23 mice by decreasing brain levels of Aβ and suppressing neurodegeneration.

The findings of the present study also demonstrate that oral administration of the EP_4 receptor-specific antagonist, AE3-208, ameliorates the spatial learning and memory deficits of APP23 mice. AE3-208 has been shown to have some therapeutically beneficial effects, including suppression of tumor growth (Terada *et al.* 2010) and suppression of autoimmune encephalomyelitis (Yao *et al.* 2009). However, it has been reported that AE3-208 exacerbates dextran sodium sulfate-induced colitis, an animal model for ulcerative colitis (Kabashima *et al.* 2002), and that a specific agonist for the EP_4 receptor stimulates bone formation and prevents bone loss (Yoshida *et al.* 2002), suggesting that EP_4 receptor antagonists, including AE3-208, have adverse effects on colitis and osteoporosis, possibilities that must be considered if these agents are to be developed for the clinical treatment of AD. Although the transitional character of orally administered AE3-208 to the brain has not yet been examined, the results of the present study suggest that it can

